



Holographic alloy positioning design system and holographic network phase diagrams of Au–Cu system

You-qing XIE^{1,2,3}, Xin-bi LIU^{1,2,3}, Xiao-bo LI⁴, Hong-jian PENG⁵, Yao-zhuang NIE⁶

1. School of Materials Science and Engineering, Central South University, Changsha 410083, China;
2. Powder Metallurgy Research Institute, Central South University, Changsha 410083, China;
3. State Key Laboratory of Powder Metallurgy, Central South University, Changsha 410083, China;
4. School of Materials Science and Engineering, Xiangtan University, Xiangtan 411105, China;
5. School of Chemistry and Chemical Engineering, Central South University, Changsha 410083, China;
6. School of Physics and Electronics, Central South University, Changsha 410083, China

Received 8 December 2014; accepted 18 January 2015

Abstract: Taking Au–Cu system as an example, three discoveries and two methods were presented. First, a new way for boosting sustainable progress of systematic metal materials science (SMMS) and alloy gene engineering (AGE) is to establish holographic alloy positioning design (HAPD) system, of which the base consists of measurement and calculation center, SMMS center, AGE center, HAPD information center and HAPD cybernation center; Second, the resonance activating-synchro alternating mechanism of atom movement may be divided into the located and oriented diffuse modes; Third, the equilibrium and subequilibrium holographic network phase diagrams are blueprints and operable platform for researchers to discover, design, manufacture and deploy advanced alloys, which are obtained respectively by the equilibrium lever numerical method and cross point numerical method of isothermal Gibbs energy curves. As clicking each network point, the holographic information of three structure levels for the designed alloy may be readily obtained: the phase constitution and fraction, phase arranging structure and properties of organization; the composition, alloy gene arranging structure and properties of each phase and the electronic structures and properties of alloy genes. It will create a new era for network designing advanced alloys.

Key words: Au–Cu system; holographic alloy positioning design system; equilibrium and subequilibrium holographic network phase diagrams; systematic metal materials science; network designing advanced alloys

1 Introduction

There exist a lot of invented advanced alloys in the alloy systems consisting of 81 kinds of metal elements accounting for 79% in the Periodic Table of Elements, that needs a new way for researchers to discover, design, manufacture and deploy advanced alloys as taking and using manpower and material resources sparingly frame. Nowadays, the old and historical biological has science why has reached to the level to be capable of transferring genes and the “clone” creature, while in the same old field of the metal materials science, alloy design is still at the stage of experimental design (or cooking method). According to the three-stage evolution of the way of thinking of human (naive holism, reductionism,

systematology or systematic holism), the development process of the metallic materials science has been analyzed [1–3], and the following main conclusions have been obtained:

1) In the past several centuries, reductionism was in dominant position in the West. Materials scientists in this period could only follow the law of historical development to establish a theory with a single-structure or a single-property. The exact reason is that the reductionism way of thinking is deep-rooted and is difficult to change, because of the long history of the metallic materials science.

2) In the middle of the 20th century, BERTALANFFY, a biologist, established general systematology. Since then, the biology was rapidly developed due to both the conflict between “holism” and

“reductionism” and the combination of “analysis” and “integration”. At that time, the material physicists believed that the development of the metallic materials science would depend on the electronic theory of alloys; the material thermo-chemists believed that the development of the materials science would depend on the thermodynamics. So far, the electron theory of alloy phases is developing along the quantum mechanical band theory → quantum mechanical ab initio calculations (QMAC)→QMAC-thermodynamics [4–11], then, the QMAC-community has been formed. The thermodynamics of alloy phases is developing along the statistic thermodynamics of alloy phases → calculation of phase diagrams (CALPHAD) → thermodynamics [12–20], then, the CALPHAD-community has been formed. However, most of the design and testing of alloys are currently performed through time-consuming and repetitive experiment. In order to discover, design, manufacture and deploy advanced materials in a more expeditious and economical way, the materials genome initiative (MGI) was proposed, where the “materials genome” was given a rather vague definition [21]. Recently, the materials genome has been defined as “a set of information (databases) allowing predication of a material’s structure, as well as its response to processing and usage conditions” [22]. We would say that it is not a good way, because the main barriers to hinder progress in thermodynamics and electron theory of alloys can not be removed by this way. First, they have not found the alloy gene (AG) sequence and AG-Gibbs energy level sequence, then the AG- Gibbs energy partition function can not be established, and the real Gibbs energy function can not be derived. Second, they have not found the reason for keeping structure stabilization of alloys against changing temperature and the atom movement mechanism to change structure for suiting variation in temperature. Third, up to now, researchers have got used to recognizing the experimental phenomena observed during very slow variation in temperature to be thermodynamic equilibrium [23–28], lacking an essential definition of the thermodynamic equilibrium order-disorder transition. Fourth, up to now, researchers have not understood that the real Gibbs energy function of an alloy phase should be derived from Gibbs energy partition function constructed of alloy gene sequences and their Gibbs energy level sequences.

3) The human way of thinking has evolved into systematic thinking mode. People become more and more clearly realized that it is important to think and deal with the complex system as a whole. The widespread of the systematic thinking mode will inevitably lead materials science to develop towards the direction of “systematization”, “high mathematization” and

“integration of science and technology”. Unfortunately, the reductionism thinking mode is still in the dominant position of metallic materials science.

Since the 1970s, we have been engaged in establishing the systematic metallic materials science (SMMS) based on the systematology, which includes system sciences, information sciences, and cybernation sciences, and gotten systematic achievements:

1) According to the systematic structure diversity proposition of systematology, which is “A diversity of structures of a system is attributed to combination and arrangement of structure units in basic structure unit sequences”, we discovered that the alloy gene (AG)-sequences are the central characteristic atom sequences in the basic coordination cluster sequences and established AG-theory based on the experimental data [29,30] or first-principles electron theory of alloys [31,32], which includes separated theory of AG-potential energies and volumes [33,34], AG-valence bound theory [35,36] and AG-thermodynamics [37].

2) According to the systematic properties diversity proposition of systematology, which is “A diversity of properties of a system is attributed to contents and transmission mode of the information about properties of basic structure unit sequences”, we established the transmission law of the extensive q -properties of alloy genes [37,38] and the AG-Gibbs energy $\Omega(x,T)$ -partition function [37], and discovered six rules for establish $\Omega(x,T)$ -partition function [39].

3) According to the systematic entirety and correlativity proposition of systematology, which is “The entirety of a complex system is attributed to the multilevel of structures and properties and to the correlatives between different structural levels, between different properties and between structures and properties”, we proposed that the SMMS framework contains three levels: the electron-structures of atoms, atom- and electron (valence bond)-structures of phases and phase-structures of organizations, which are simplified as atom-level, phase-level and organization-level, respectively [37].

4) According to the systematic openness proposition of systematology, which is “Properties are determined by structure; properties should be suitable for environments; environments change structure”, we pointed out that the man’s knowledge of relationships of structures, properties and temperature for alloys has been changed from single causality to systematic correlativity. We also discovered that the systematic correlativity may be described by a set of equilibrium holographic network phase (EHNP) diagrams of each ordered sublattice system and discovered system, which belong in contents of the alloy gene arranging (AGA) theory of alloy phases.

The AGA-theory includes AGA-equilibrium thermodynamics [37–39], AGA-subequilibrium thermodynamics [40], AGA-crystallography [40,41], and AGA-valence bond theory [43–46]. Then, we established a set of equilibrium holographic network phase (EHNP) diagrams of AuCu-, AuCu₃- and Au₃Cu-type sublattice systems by the minimum mixed Gibbs energy path method (see Appendix A.3).

5) According to the systematic kinetics proposition of systematology, which is “A system has not only ability to keep structure stabilization against a changing environment, but also a mechanism to change structure for suiting variation in environments”, taking experimental path on disordering AuCuI ($A_8^{\text{Au}} A_4^{\text{Cu}}$) composed of A_8^{Au} and A_4^{Cu} stem alloy genes as an example, we presented three discoveries and a method. The ability of AuCuI ($A_8^{\text{Au}} A_4^{\text{Cu}}$) to keep structure stabilization against changing temperature is attributed to the fact that the A_8^{Au} and A_4^{Cu} potential well depths greatly surpass their vibration energies, which leads to the subequilibrium of experimental path; A new atom movement mechanism of AuCuI ($A_8^{\text{Au}} A_4^{\text{Cu}}$) to change structure for suiting variation in temperature is the “resonance activating-synchro alternating” (RA-SA) of alloy genes, which leads to heterogeneous and successive subequilibrium transitions; There exists jumping order degree, which leads to the existence of jumping T_j -temperature and an unexpected so-called “retro-effect” about jumping temperature retrograde shift to lower temperatures upon increasing the heating rate. A set of subequilibrium holographic network path charts have been obtained by the experimental mixed enthalpy path method [40].

6) According to the sixth and seventh systematic philosophic propositions of systematology proposed in this work, one of them is that “The vitality of a system is attributed to information cycle” (simplified as systematic vitality proposition or systematic information cycle proposition), the other is that “The entire optimization of a system is attributed to effective cybernation” (simplified as the systematic entire optimization proposition or systematic cybernation proposition), we have discovered that the new way for boosting sustainable progress of SMMS and alloy gene engineering (AGE) is to establish HAPD-system of alloy systems, of which the base consists of measurement and calculation (MC) center, SMMS center, AGE center, HAPD-system information center and HAPD-system cybernation center. The equilibrium and subequilibrium holographic network phase (EHNP and SHNP) diagrams are the blueprints and operable platform for researchers to discover, design, manufacture and deploy advanced alloys. In this work, we take Au–Cu order-disorder system as an example to present HAPD-system base,

EHNP- and SHNP-diagrams.

2 HAPD-system base

The HAPD-system is a three-in-one combination body composed of the science, technology and social engineering, which includes three levels: 1) HAPD-system science consisting of the SMMS-framework, HAPD-system information (HAPDSI) science and HAPD-system cybernation (HAPDSC) science, as well as philosophy; 2) HAPD-system technology engineering (simplified as AG-engineering) consisting of discovery, design, certification and manufacture technologies; 3) HAPD-system base consisting of MC-center, SMMS-center, AGE-center, HAPDSI-center and HAPDSC-center. Their systematic correlativity may be explained by HAPD-system base.

2.1 MC-center and SMMS-center

The SMMS-framework is established by complete scientific theory research stages: experimental observation and measurements–perceptual knowledge–image thinking–mathematics thinking–information circulation–philosophic thinking. There may have new discovers and innovative achievements obtained at every stage, but experimental observation and measurements are still the source of theory innovation and the criterion for test theory, and the philosophy is the “mother” of all sciences, because the functions of the philosophy in the scientific practice are not only to explain and guide, but also to strengthen the scientific faith and courage of the explorers. It is a good example that the old and historical metal materials science has been developed into the SMMS-framework.

The MC-center is responsible for chemical analysis (CA), structure and property (SP) measurements and applied analogy, as well as computer calculation. It has been realized that the operable platform for researchers to discover, design, manufacture and computer programs, capacity and instrument (see Fig. 1(a)).

The SMMS-framework consists of three level theories: AG-theory, AGA-theory and alloy phase arranging (APA) theory. Similar to any other system, each structure level theory has its constituent units, structure units, structure model, mathematic equations, information circulation, scientific functions and scientific significance.

The SMMS-center is the basic part of the HAPD-system (see Fig. 1(b)). The main tasks of the SMMS-center are to develop SMMS-framework and to establish holographic alloy knowledge (HAK) database of alloy systems.

2.1.1 Developing AG-theory and establishing AG-database

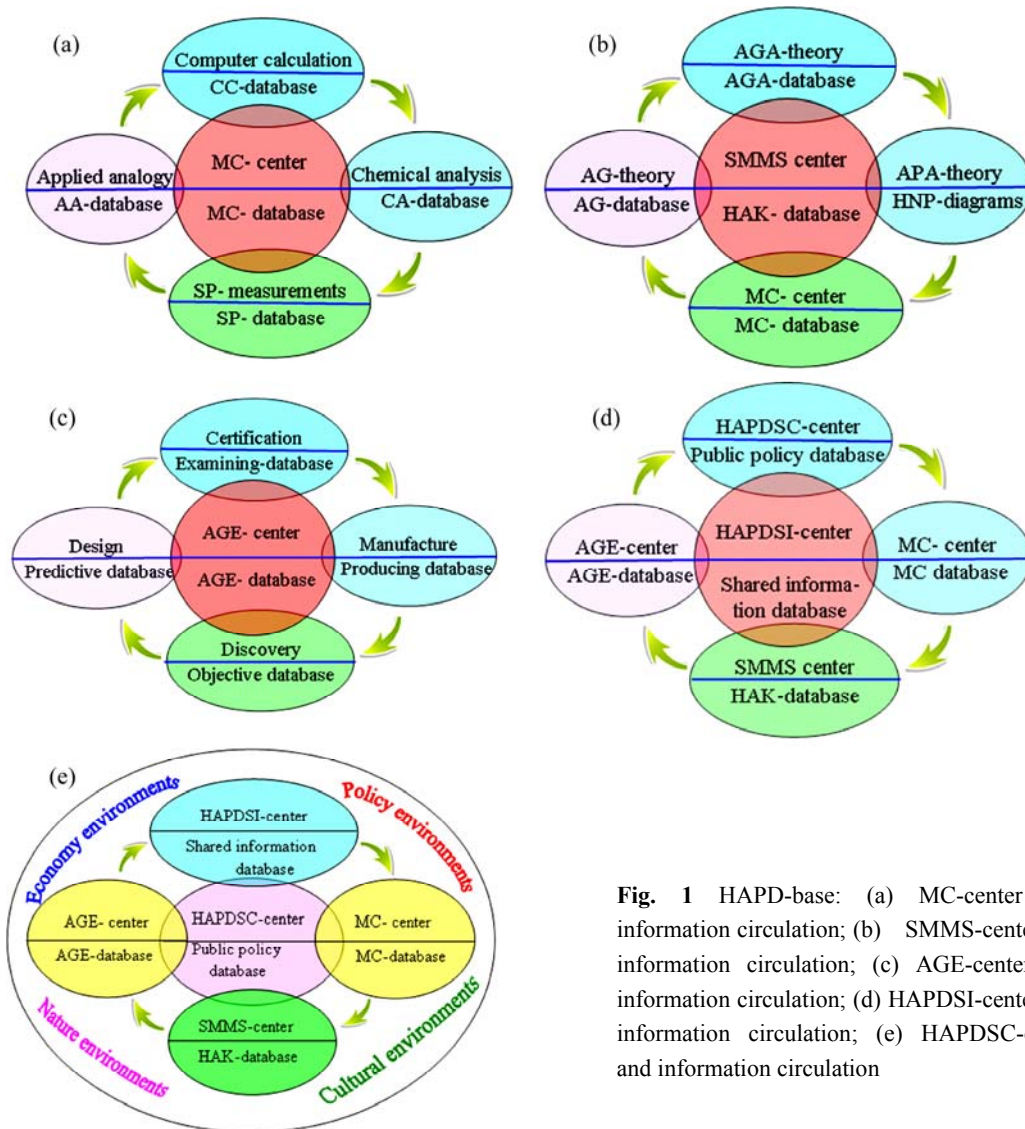


Fig. 1 HAPD-base: (a) MC-center and information circulation; (b) SMMS-center and information circulation; (c) AGE-center and information circulation; (d) HAPDSI-center and information circulation; (e) HAPDSC-center and information circulation

While forming alloy by pure elements, it is a fact without dispute that constituent atom states split into the atomic state sequences, due to the influence of the coordinative configurations. Therefore, the central characteristic atom sequences in the coordination cluster sequences should be taken as the basic structure unit sequences, i.e., AG-sequences. Analogously with the biological gene, an alloy gene sequence is defined as a characteristic atom sequence carrying a set of transmission information about electronic structures, physical and thermodynamic properties, which may be obtained by AG-theory [37]. Therefore, the alloy gene and characteristic atom are synonym. To develop AG-theory and establish AG-database of binary and ternary alloy systems is not only a long-term but also tough task, that needs the cooperation of scientists and engineers in the world.

2.1.2 Developing AGA-theory and establishing AGA-database

The establishments of the AG-theory and AG-holographic information database have led traditional alloy phase theories to fundamental variations. 1) Based on the AG-holographic information database, the crystallography described by constituent atoms occupied at lattice points has been developed into the AGA-crystallography described by alloy genes-occupied at lattice points [41,42]. 2) Based on the AG-Gibbs energy levels, the statistic thermodynamics described by constituent atoms pairs and constituent atoms clusters, of which the constituent atoms occupied at lattice points, has been developed into the AGA-equilibrium thermodynamics described by alloy genes occupied at the AG-Gibbs energy levels [37–39]. 3) Based on the AG-valence electron structure sequences, the first principle electron theory of alloys has been developed into the AGA-valence bond theory of alloy phases [43–46]. 4) Based on the RA-SA mechanism and experimental path tracking method, the AGA-kinetics of

the order-disorder transition described by AGA-holographic network path charts has been established [40]. 5) Based on the AG-holographic information database and essential definition of equilibrium order-disorder transition, the traditional phase diagram of single ordered phase sublattice system described only by phase boundary lines has been developed into a set of EHNP-diagrams described by a set of information about AGA-structures, physical and thermodynamic properties [37–39]. 6) Based on the AG-holographic information database and essential definition of subequilibrium order-disorder transition, the SHNP-diagrams of single ordered phase sublattice system described by a set of information about AG-concentrations, physical and thermodynamic properties may be established (see Section 4). However, to develop AGA-theory and establish AGA-database of binary and ternary alloy systems is not only a long-term but also a tough task, which needs cooperation of scientists and engineers in the world.

2.1.3 Developing APA-theory and establishing APA-database

The APA-theory in the SMMS-framework includes APA-equilibrium thermodynamics, APA-subequilibrium thermodynamics and APA-structure theory. The main task of APA-equilibrium thermodynamics is to establish EHNP-diagrams of alloy systems (see Section 3). The main task of APA-subequilibrium thermodynamics is to establish SHNP-diagrams of alloy systems, which are proposed in the present research work (see Section 4).

The complete scientific theory research stages are completed by different scientists and engineers at different stages of the process, but their results, knowledge, achievements and so on should be deposited into the holographic alloy knowledge (HAK) database to be shared for scientists and engineers, that is very useful to accelerate the full continuum.

2.2 AGE-center

The wide spread of the systematic thinking mode will inevitably lead materials science to develop towards the direction of integration of science and technology, which is one of the characters of the “big science”. Science is the source of all technological achievements, and the development of science is also dependent on the progress of technology. The main tasks of AGE-center are to obtain advanced materials and to establish AGE-information database. In general, an advanced material from conception to market deployment should undergo four stages (Fig. 1(b)): discovery → design → certification → manufacturing, which may be completed by different scientific and engineering teams at different stages of the process, but their inventive stories, design procedures, certification examinations, technological

process, deployment results and so on should be deposited into the AGE-information database to be shared for scientists and engineers, that is very useful to accelerate the full continuum.

2.3 HAPDSI-center

“A vitality of a system is attributed to information circulation”. Early in 2003, we advocated to establish metallic materials information science, which is focused on both the rebirth of general information and objective information and the running rules of their expression, transform, storage, transform, examination and results. In order to strengthen motive force of sustainable progress of systematic metal materials science and alloy gene engineering, it is necessary to establish HAPSI-center, which is a hub of information in the HAPD-system. Its main tasks are as follows: 1) To establish MC-database and shared information platform, through cooperation with the MC-center; 2) To establish shared HAK-database and shared information platform, through cooperation with the SMMS-center; 3) To establish AGE-database and shared information platform, through cooperation with the AGE-center; 4) To establish public policy database and platform, through cooperation with the HAPSC-center; 5) To establish shared information database and platform in the HAPSI-center for serving scientists, engineers and staff members in the HAPDS-base; 6) To increase, check and correct information, through information cycle and cooperation with other centers.

2.4 HAPDSC-center

“The entire optimization of a system is attributed to effective cybernation”. In essence, the HAPDS-base is a science–technology–society combination body established along the route of science–technology–manufacture–deploy–development. The development is responsible for the fact that the achievements of science and technology are directly turned productive force in society and that the wider support is won from society. The society includes policy environment, economy environment, culture environment and nature environment. In order to discover, design, manufacture and deploy advanced alloys in a more expeditions and economical way, it is necessary to establish HAPSC-center, which is a hub of cybernation in the HAPDS-base (Fig. 1(e)). Besides, to be responsible for development, HAPDSC-center should be responsible for the following tasks: 1) The immediate and long-term objective programs of the HAPDS-base and several centers should be drawn up, through cooperation with other centers; 2) The running rules and regulations of the HAPDS-base and several centers should be drawn up,

through cooperation with other centers; 3) In order to realize objectives for supplying society demands in a more expeditious and economical way, the HAPDS-base should keep in overall optimization, through adjusting systematic structure and adopting various measures based on analysis of the cycling information; 4) The HAPDSC-center should be responsible for drawing up train regulation of researchers, engineers and staff members, that is a fundamental cybernation measure to realize objectives, because they are basic structure unit sequences of the HAPDS-base.

3 EHNP-diagram of Au–Cu system

Since 1916, the pioneering work of KURNAKOV et al, the FCC-based lattice Au–Cu system with ordered Au₃Cu-, AuCu- and AuCu₃-type sublattice systems, as well as disordered FCC-based lattice system have been studied as a classical paragon with complete order–disorder transition for about a centenary. However, a real equilibrium phase diagram of Au–Cu system has not been established, because one of many reasons is that researchers have got used to recognizing experimental phenomena observed during very slow variation in temperature to be thermodynamic equilibrium phenomena: 1) The middle jumping T_j -temperatures are erroneously considered as the terminal T_c -critical temperatures of equilibrium order-disorder transition of alloys, although the experimental jumping σ_j -order degrees are 0.8–0.6 and the experimental short range order degrees exist at the temperatures considerable above the T_j -temperature [23,28]. 2) The composition-dependent T_i - x curve is erroneously considered as the phase boundary T_c - x curve of phase diagram [17,18,50,51]. 3) The heterogeneous “subequilibrium statistic region-scale heterogeneity” with the same composition and different order degrees is erroneously considered as two heterogeneous “equilibrium two-phase region” consisting of ordered and disordered phases. It means that the equilibrium diagram would show the ordered phase separated from the disordered phase by a two-phase region [24]. 4) They hold that the stoichiometric Au₃Cu-, AuCu- and AuCu₃- compounds in the Au₃Cu-, AuCu- and AuCu₃-type sublattice systems have the lowest potential energies at 0 K and the highest T_c -critical temperatures on their phase boundary curves, respectively. The researchers in the CALPHAD- and QMAC-communities took these miss understandings of experimental phenomena as the selected information, then adjusted parameters in Gibbs energy functions (or wave functions and potential functions within the local-density- functional formalism) and established so-called equilibrium phase diagrams to achieve the best representation of the selected information [22]. These

phase diagrams are questionable in many respects (see Appendix A.1).

The main task of APA-equilibrium thermodynamics is to establish EHNP-diagrams of alloy systems with multi-phases competition. The essential definition of equilibrium order-disorder transition is that “the AG- Gibbs energy levels ($G_i^{\text{Au}}(T)$, $G_i^{\text{Cu}}(T)$) and AG-probabilities ($x_i^{\text{Au}}(x, T, \sigma)$, $x_i^{\text{Cu}}(x, T, \sigma)$) occupied at the $G_i^{\text{Au}}(T)$ - and $G_i^{\text{Cu}}(T)$ - energy levels can respond immediately and change synchronously with each small variation in temperature and proceed along the minimal Gibbs energy path, supposing that there is no obstacle to atom movement”.

According to the essential definition of equilibrium order-disorder transition, the isothermal ΔG_T^m - x network phase diagrams of the ordered AuCu-type, AuCu₃-type and Au₃Cu-type sublattice systems, as well as FCC-based lattice disordered Au–Cu system were established [37–39].

According to steps for establishing EHNP diagrams of Au–Cu system (see Appendix A.2), the three dimensional q - T - x EHNP-diagrams, and the two dimensional T_q - x , q_T - x and q_x - T EHNP-diagrams of Au-Cu system may be established by the equilibrium lever numerical method of isothermal Gibbs energy ΔG_T^m - x curves (see Appendix B), where q denotes the mixed Gibbs energy ΔG^m , order degree σ , configurational entropy S^c , mixed characteristic Gibbs energy ΔG^{*m} , mixed enthalpy ΔH^m , mixed potential energy ΔE^m , mixed volume ΔV^m , generalized vibration free energy X^v , generalized vibration energy U^v , generalized vibration entropy S^v , mixed specific heat capacity Δc_p^m , mixed thermal expansion coefficient $\Delta \alpha^m$ and activities (a_{Au} and a_{Cu}). The $T_{\Delta G^m}$ - x and T_σ - x EHNP diagrams are respectively shown in Figs. 2 and 3 (The EHNP diagrams of other properties have been omitted), from which the following main characteristics are presented.

The ordered phases of Au₃Cu-, AuCu- and AuCu₃-type sublattice systems are separated from the disordered phase by a single T_c - x curve rather than by a two-phase coexisted region, which may be demonstrated by equilibrium lever numerical method of isothermal Gibbs energy curves (see Appendix B). This situation is attributed to the fact that the ordered and disordered phases are constructed by the same A_i^{Au} and A_i^{Cu} alloy gene sequences and the same G_i^{Au} and G_i^{Cu} Gibbs energy sequences.

The highest critical T_c -point on the T_c - x curve of Au–Cu system is located at the network point ($x_{\text{Cu}}=55.5\%$, $T_c=839$ K, $\Delta G^m=-10189.02$ J/mol), through accurate calculation by the differential method between Gibbs energies of ordered and disordered alloys

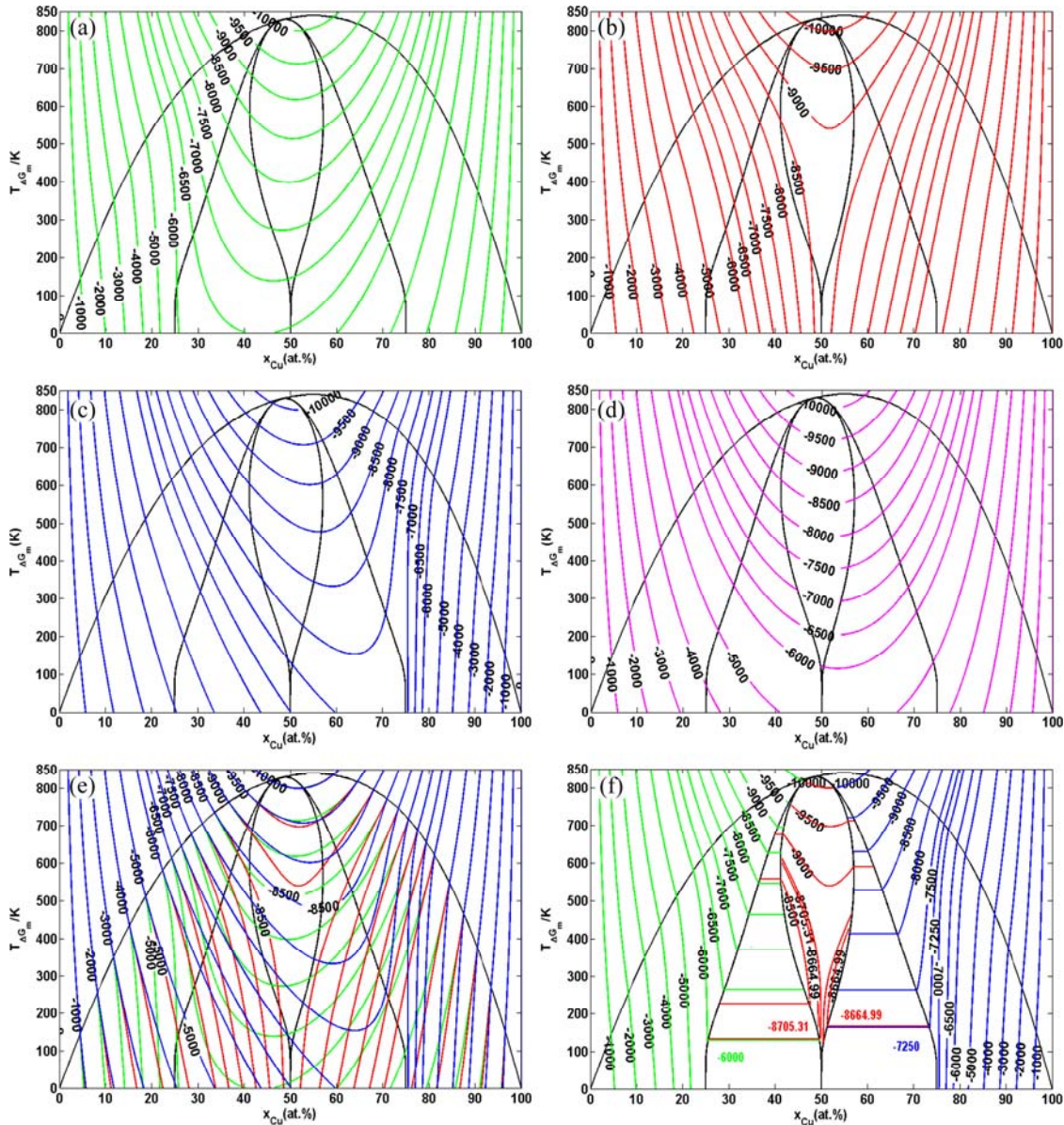


Fig. 2 $T-x$ EHPN diagrams with iso-mixed Gibbs energy $T_{\Delta G^m} - x$ curves of Au–Cu system: (a) Equilibrium phase diagram with iso-mixed Gibbs energy $T_{\Delta G^m} - x$ curves of Au_3Cu -type sublattice system; (b) Equilibrium phase diagram with iso-mixed Gibbs energy $T_{\Delta G^m} - x$ curves of AuCu-type sublattice system; (c) Equilibrium phase diagram with iso-mixed Gibbs energy $T_{\Delta G^m} - x$ curves of AuCu_3 -type sublattice system; (d) Equilibrium phase diagram with iso-mixed Gibbs energy $T_{\Delta G^m} - x$ curves of FCC-based lattice disordered $\text{Au}_{(1-x)}\text{Cu}_x$ solution; (e) Equilibrium phase diagram with iso-mixed Gibbs energy $T_{\Delta G^m} - x$ curves of Au_3Cu -, AuCu- and AuCu_3 -type sublattice systems described by green, red and blue curves respectively; (f) Equilibrium phase diagram of Au–Cu system with iso-mixed Gibbs energy $T_{\Delta G^m} - x$ curves and equilibrium isothermal Gibbs energy levels

(see Appendix C).

There exist phase boundary curves with two-phase coexisting regions between the two ordered phases. The two-phase coexisting region between the Au_3Cu - and AuCu-type ordered alloy phases is described by $[T_{\Delta G^m}(\text{Au}_3\text{Cu} - \text{type}) - x]_{\text{PB}}$ and $[T_{\Delta G^m}(\text{AuCu} - \text{type}) - x]_{\text{PB}}$ phase boundary curves (left side on Fig. 2(f)). The two-phase coexisting region between the AuCu- and AuCu_3 -type ordered alloy phases is described by $[T_{\Delta G^m}(\text{AuCu} - \text{type}) - x]_{\text{PB}}$ and $[T_{\Delta G^m}(\text{AuCu}_3 - \text{type}) -$

$x]_{\text{PB}}$ phase boundary curves (right side on Fig. 2(f)). In the single- and two-phase regions, a lot of information may be obtained, as clicking any one network point: 1) The phases and their fractions, average Gibbs energy and average other properties of the alloy at this network point are present; 2) The compositions, Gibbs energies, a set of thermodynamic properties, AGA-structures and their properties of the phases are present, because all $q-T-x$ EHPN-diagrams are interlinked.

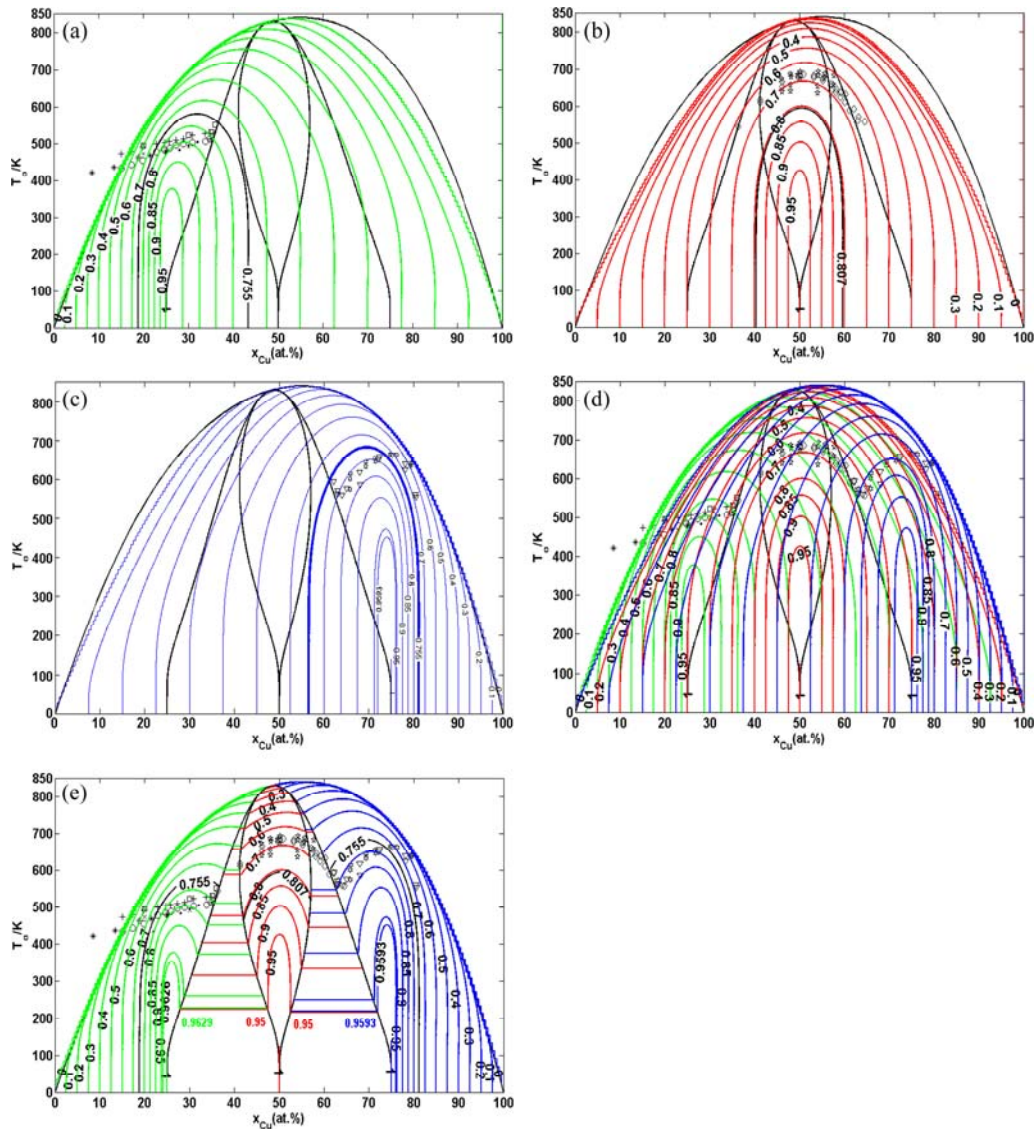


Fig. 3 T - x EHNPs diagrams with iso-order degree T_σ - x curves of Au–Cu system: (a) Equilibrium phase diagram with iso-order degree T_σ - x curves of Au_3Cu -type sublattice system; (b) Equilibrium phase diagram with iso-order degree T_σ - x curves of AuCu -type sublattice system; (c) Equilibrium phase diagram with iso-order degree T_σ - x curves of AuCu_3 -type sublattice system; (d) Equilibrium phase diagram with iso-order degree T_σ - x curves of Au_3Cu -, AuCu - and AuCu_3 -type sublattice systems described by green, red and blue curves, respectively; (e) Equilibrium phase diagram with iso-order degree T_σ - x curves (The experimental jumping $T_j(x)$ points were erroneously considered as the equilibrium critical $T_c(x)$ points, which are introduced from references given in [17])

4 SHNP-diagrams of Au–Cu system

The main task of APA-subequilibrium thermodynamics is to establish SHNP-diagrams. The essential definition of subequilibrium order→disorder transition is that “the AG-Gibbs energy levels can respond immediately with each small variation in temperature, but the AG-probabilities occupied at the AG-Gibbs energy levels can not change synchronously, even by extremely slow heating (or cooling) rate, which leads to the fact that its Gibbs energy path is higher than equilibrium path”. We discovered that this transition needs superheated (or supercooled) driving Gibbs energy

together with atom movement RA-SA mechanism. It means that the alloy system is at subequilibrium, of which the Gibbs energy is not at the minimum under some specified combination of temperature and composition, but the characteristics of the SHNP-diagrams do not change nearly with time, which may be several months, several years and even several decades.

According to steps for establishing SHNP diagrams of Au–Cu system (see Appendix A.2), the three dimensional q - x - T EHNPs-diagrams, and the two dimensional T_q - x , q_T - x and q_x - T EHNPs-diagrams of Au–Cu system may be established by the subequilibrium cross point numerical method (or differential method) of isothermal Gibbs energy

$\Delta G_T^m - x$ curves (see Appendix C), where q denotes mixed Gibbs energy ΔG^m , order degree σ , configurational entropy S^c , mixed characteristic Gibbs energy ΔG^{*m} , mixed enthalpy ΔH^m , mixed potential energy ΔE^m , mixed volume ΔV^m , generalized vibration free energy X^V , generalized vibration energy U^V , generalized vibration entropy S^V , mixed specific heat capacity ΔC_p^m , mixed thermal expansion coefficient $\Delta\alpha^m$ and activities (a_{Au} and a_{Cu}). The $T_{\Delta G^m} - x$ and $T_\sigma - x$ SHNP diagrams are respectively shown in Figs. 4 and 5, from which the following main characteristics are presented. We have discovered that the RA-SA mechanism is a located atom movement

mechanism rather than a oriented diffuse atom movement mechanism in the Au–Cu system, which was used to explain the heterogeneous subequilibrium successive transitions on disordering $AuCuI(A_8^{Au} A_4^{Cu})$, because the Gibbs energy differences between $AuCu$ - and Au_3Cu -type ordered alloys and between $AuCu$ - and $AuCu_3$ -type ordered alloys are small and the volume differences between A_i^{Au} and A_i^{Cu} alloy genes are very large. Therefore, we have predicated the subequilibrium limit composition ranges of the long range ordered (LRO) Au_3Cu -, $AuCu$ - and $AuCu_3$ -type alloys at 0 K (see Fig. 5(f)). 1) The subequilibrium limit composition range of the LRO Au_3Cu -type alloys is the

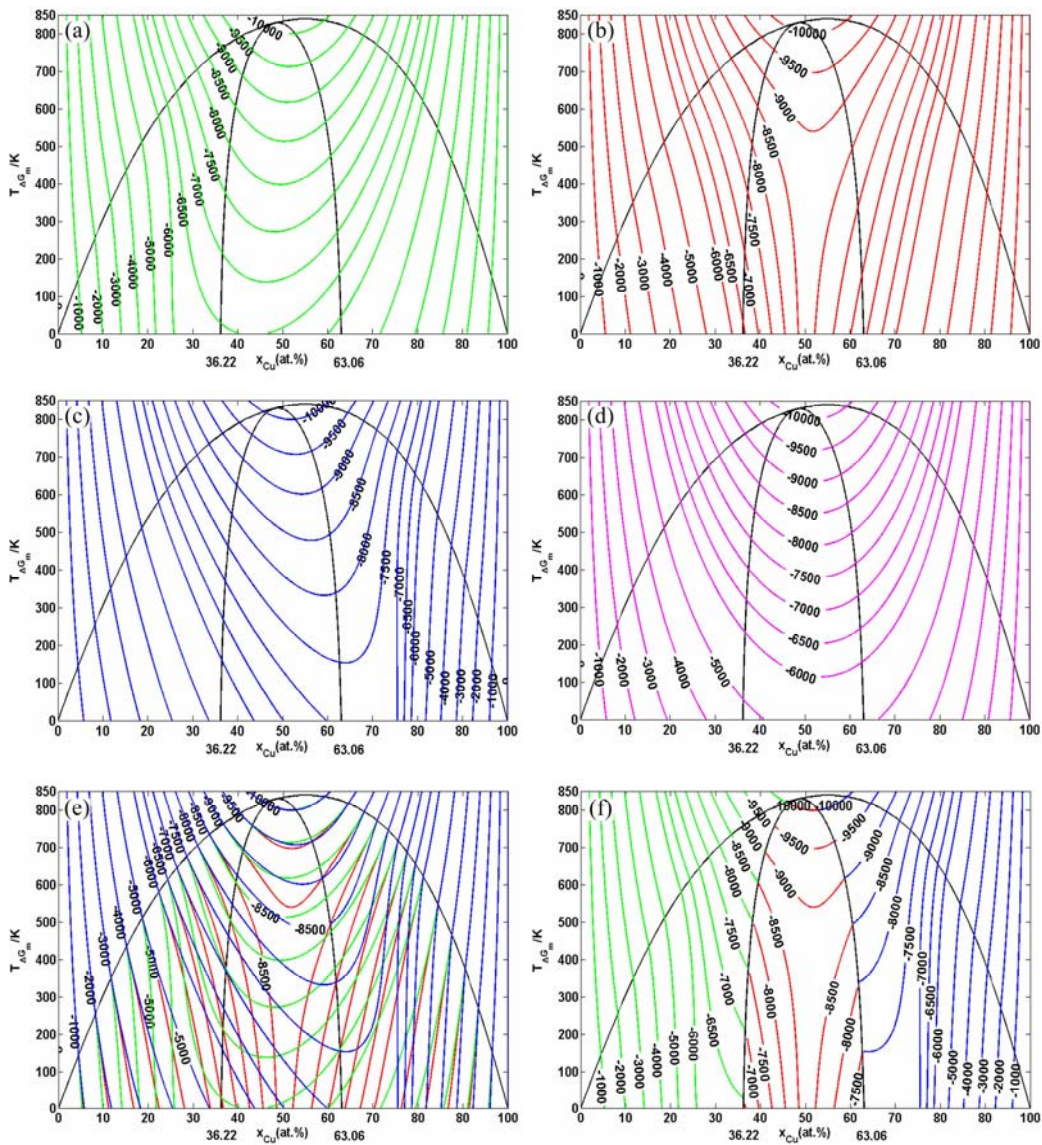


Fig. 4 T - x SHNP diagrams with iso-mixed Gibbs energy $T_{\Delta G^m} - x$ curves of Au–Cu system: (a) Subequilibrium phase diagram with iso-mixed Gibbs energy $T_{\Delta G^m} - x$ curves of Au_3Cu -type sublattice system; (b) Subequilibrium phase diagram with iso-mixed Gibbs energy $T_{\Delta G^m} - x$ curves of $AuCu$ -type sublattice system; (c) Subequilibrium phase diagram with iso-mixed Gibbs energy $T_{\Delta G^m} - x$ curves of $AuCu_3$ -type sublattice system; (d) Subequilibrium phase diagram with iso-mixed Gibbs energy $T_{\Delta G^m} - x$ curves of FCC-based lattice disordered $Au_{(1-x)}Cu_x$ solution; (e) Subequilibrium phase diagram with iso-mixed Gibbs energy $T_{\Delta G^m} - x$ curves of Au_3Cu -, $AuCu$ - and $AuCu_3$ -type sublattice systems described green, red and blue curves respectively; (f) Subequilibrium phase diagram of Au–Cu system with iso-mixed Gibbs energy $T_{\Delta G^m} - x$ curves

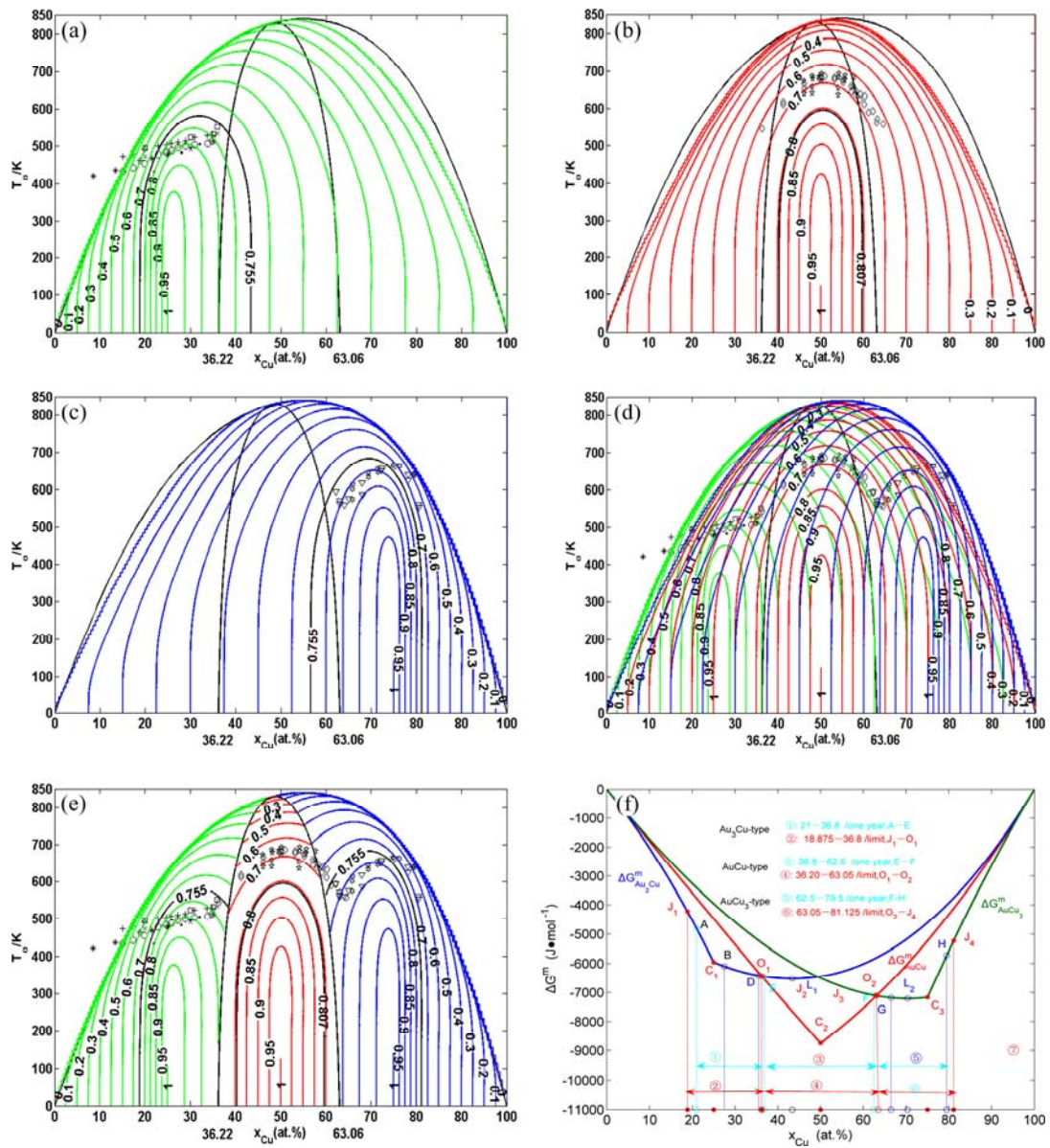


Fig. 5 $T-x$ SHNP diagrams with iso-order degree $T_\sigma-x$ curves of Au-Cu system: (a) Subequilibrium phase diagram of Au-Cu system with iso-order degree $T_\sigma-x$ curves of Au_3Cu -type sublattice system; (b) Subequilibrium phase diagram of Au-Cu system with iso-order degree $T_\sigma-x$ curves of AuCu-type sublattice system; (c) Subequilibrium phase diagram of Au-Cu system with iso-order degree $T_\sigma-x$ curves of $AuCu_3$ -type sublattice system; (d) Subequilibrium phase diagram of Au-Cu system with iso-order degree $T_\sigma-x$ curves of Au_3Cu -, AuCu- and $AuCu_3$ -type sublattice systems, described by the green, red and blue curves, respectively; (e) Subequilibrium phase diagram of Au-Cu system with iso-order degree $T_\sigma-x$ curves of Au-Cu system; (f) Characteristics of $\Delta G_{Au_3Cu}^m-x$, ΔG_{AuCu}^m-x and $\Delta G_{AuCu_3}^m-x$ curves of Au_3Cu -type, AuCu-type and $AuCu_3$ -type sublattice systems at 0 K. Each point is described by composition, mixed Gibbs energy and order degree: $J_1(18.875, -4220.47, 0.0.7540)$, $A(21.00, -4807.10, 0.8400)$, $C_1(25.00, -5955.72, 1)$, $B(27.50, -6094.93, 0.9667)$, $D(35.50, -6411.03, 0.8600)$, $O_1(36.20, -6428.97, 0.8507)$, $E(36.80, -6443.06, 0.8427)$, $J_2(43.375, -6518.13, 0.7553)$, $L_1(43.40, -6518.13, 0.7547)$, $C_2(50, -8746.23, 1)$, $J_3(56.625, 0.7547)$, $F(62.50, -7094.10, 0.8333)$, $O_2(63.05, -7108.69, 0.8407)$, $G(66.50, -7176.61, 0.8667)$, $L_2(70.35, -7203.16, 0.9380)$, $C_3(75, -7163.61, 1)$, $H(79.50, -5726.05, 0.8200)$, $J_4(81.125, -5320.59, 0.7550)$ (The experimental jumping $T_j(x)$ points were erroneously considered as the equilibrium critical $T_c(x)$ points, which are introduced from references given in [17])

J_1-O_1 range: 18.875%–36.20% Cu at 0 K, where the down-composition J_1 -point is determined by the first jumping order degree (0.755) of the jumping A_5^{Au} - alloy gene in the Au_3Cu -type sublattice system [38], and the

O_1 -point is determined by the cross point of isothermal Gibbs energy curves between AuCu- and Au_3Cu -type ordered alloys. 2) The subequilibrium limit composition range of the LRO $AuCu_3$ -type alloys is the O_2-J_4 range:

63.05%–81.125% Cu at 0 K, where the up-composition J_4 -point is determined by the first jumping order degree (0.755) of the jumping A_7^{Cu} -alloy gene in the AuCu_3 -type sublattice system [39], and the O_2 -point is determined by the cross point of isothermal Gibbs energy curves between AuCu - and AuCu_3 -type ordered alloys at 0 K. 3) The subequilibrium limit composition range of the LRO- AuCu -type alloys is the O_1 - O_2 range: 36.20%–63.05% Cu at 0 K, which is in excellent agreement with the experimental range 36.8%–62.5% Cu [47–49].

It has been also predicated that the $T_{\Delta G^m} - x$ and $T_{\sigma} - x$ SHNP diagrams of Au-Cu system should be established by the cross point numerical method (or differential numerical method) of equilibrium isothermal Gibbs energy $\Delta G_T^m - x$ curves (see Figs. 4 and 5, and Appendix C). 1) The phase boundary curves between ordered region and disordered region are the joining point $T_c - x$ curves of isothermal Gibbs energy curves. 2) The phase boundary curves between AuCu - and Au_3Cu -type ordered regions and between AuCu - and AuCu_3 -type ordered regions are respectively the $[T_{\Delta G^m}(\text{Au}_3\text{Cu} - \text{type}, \text{AuCu} - \text{type}) - x]_{\text{PB}}$ curve (left side on Fig. 4(f)) and $[T_{\Delta G^m}(\text{AuCu} - \text{type}, \text{AuCu}_3 - \text{type}) - x]_{\text{PB}}$ curve (right side on Fig. 4(f)) in the $T_{\Delta G^m} - x$ SHNP diagrams.

We have discovered that the first and second jumping alloy genes and their jumping order degrees depend on the compositions of alloys. For examples, in the stoichiometric ordered AuCu_3 alloy, they are respectively $A_{j,7}^{\text{Cu}}$ with $\sigma_j = 0.750$ and $A_{j,11}^{\text{Au}}$ with $\sigma_j = 0.730$; in the ordered $\text{Au}_{22}\text{Cu}_{78}$ alloy, they are respectively $A_{j,9}^{\text{Cu}}$ with $\sigma_j = 0.792$ and $A_{j,11}^{\text{Au}}$ with $\sigma_j = 0.616$. The details will be presented in another paper. Therefore, it has been predicated that there exist jumping iso-order degree $T_{\sigma_j} - x$ regions in the range $0.6 \leq \sigma_j(x, T) \leq 0.8$. It means that there exist LRO-regions, SRO (short range ordered)-regions and disordered region in the SHNP diagrams of Au-Cu system. These predications above have been demonstrated to be in good agreement with the experimental phenomena (see Figs. 5(a)–(d)).

We also predicated that the phase boundary curves between two ordered phases may be possible to expand into the narrow coexisted phase boundary bands of two ordered phases via proper heat treatment or very long ageing. Namely, there may be decomposition reaction:

$$[T_{\Delta G^m}(\text{Au}_3\text{Cu} - \text{type}, \text{AuCu} - \text{type}) - x]_{\text{PB}} \rightarrow$$

$$[T_{\Delta G^m}(\text{Au}_3\text{Cu} - \text{type}) - x]_{\text{PB}} +$$

$$[T_{\Delta G^m}(\text{AuCu} - \text{type}) - x]_{\text{PB}}.$$

$$[T_{\Delta G^m}(\text{AuCu} - \text{type}, \text{AuCu}_3\text{type}) - x]_{\text{PB}} \rightarrow$$

$$[T_{\Delta G^m}(\text{AuCu} - \text{type}) - x]_{\text{PB}} +$$

$$[T_{\Delta G^m}(\text{AuCu}_3 - \text{type}) - x]_{\text{PB}}$$

It is often the case that the structures, properties and order–disorder transition paths and phase regions of SHNP diagrams are more describable than those associated with EHNP diagrams, which may be illustrated by the following experimental phenomena: 1) Under the experimental condition of one year of heat treatment [47–49], the composition ranges of the LRO Au_3Cu -, AuCu - and AuCu_3 -type alloys at room temperature are respectively $A-E$: 21%–36.8% Cu, $E-F$: 36.8%–62.5% Cu and $F-H$: 62.5–79.5% Cu, that approach to the predicated limit composition ranges (see Fig. 5(f)). 2) At high temperatures, the all experimental jumping $T_i(x)$ -temperatures of the LRO Au_3Cu -, AuCu - and AuCu_3 -type alloys fall within range from $T_{\sigma=0.80} - x$ curve to $T_{\sigma=0.60} - x$ curve, although they are dependent on heating rates and compositions of alloys.

5 Discussion

The Au-Cu system with complete order–disorder transition has been considered the classic paragon studied nearly by all conventional and modern measurement methods and all alloy theories for about a century. These experimental data and theoretical achievements have laid a treasure foundation for establishing SMMS-framework, which includes many new concepts and discoveries.

5.1 Relationship between EHNP and SHNP diagrams of Au-Cu system

Even though it is often the case that the structures, properties and order–disorder transition paths of SHNP charts and phase regions of SHNP diagrams are more describable than those associated with EHNP charts and EHNP diagrams, which are nevertheless useful in following aspects.

The SHNP diagrams of Au-Cu system are established by the cross point numerical method (or differential method) of equilibrium isothermal Gibbs energy $\Delta G_T^m - x$ curves in the $\Delta G^m - T - x$ EHNP diagrams of the Au_3Cu -, AuCu - and AuCu_3 -type sublattice systems, as well as FCC-based lattice disordered system. It means that “if there are no EHNP-diagrams, then there are no SHNP diagrams”.

The EHNP-diagrams may be used to understand the development and preservation of structures and their attendant properties of subequilibrium alloys in the SHNP diagrams, that may be illustrated by relationships between the EHNP and SHNP charts on disordering AuCuI ($A_8^{\text{Au}}A_4^{\text{Cu}}$) compound [40]. It may be said that “If

there are no EHNP-charts, then there are no SHNP-charts and no so much discoveries”.

Taking essential definition of equilibrium order–disorder transition as the standard, the essential definition of subequilibrium order–disorder transition has been proposed (see Sections 3 and 4).

Taking equilibrium network chart of iso-order degree mixed enthalpy $\Delta H_{e,\sigma}^m - T$ curves on disordering AuCuI ($A_8^{\text{Au}}A_4^{\text{Cu}}$) as standard, the SHNP charts on disordering AuCuI ($A_8^{\text{Au}}A_4^{\text{Cu}}$) have been obtained by the experimental mixed enthalpy $\Delta H_s^m - T$ path method, and then the SHNP charts of other ordered $\text{Au}_{(1-x)}\text{Cu}_x$ alloys in the whole composition range may be obtained by the same method.

Comparing the equilibrium $\Delta G_e^m - T$ path of equiatomic AuCu alloy with its experimental $\Delta G_s^m - T$ path, some discoveries were obtained. 1) It has been discovered that it is necessary to propose subequilibrium concept to describe the state of AuCuI ($A_8^{\text{Au}}A_4^{\text{Cu}}$) compound with higher Gibbs energy than that of equilibrium state in the temperature range $0 \text{ K} \leq T \leq T_{\text{onset}}$ (598 K), which is attributed to the fact that the A_8^{Au} - and A_4^{Cu} -alloy genes are still occupied at the $G_8^{\text{Au}}(T)$ - and $G_4^{\text{Cu}}(T)$ - Gibbs energy level, respectively, although $G_i^{\text{Au}}(T)$ and $G_i^{\text{Cu}}(T)$ sequences have changed with temperatures. 2) It has been discovered that the ability of AuCuI ($A_8^{\text{Au}}A_4^{\text{Cu}}$) to keep structure stabilization against changing temperature is attributed to the fact that the AG-potential well depths greatly surpass superheated driving Gibbs energy and AG-vibration energies. Even at the $T_{\text{onset}} = 598 \text{ K}$, $|U_8^{\text{Au,v}}/E_8^{\text{Au}}|$ and $|U_4^{\text{Cu,v}}/E_4^{\text{Cu}}|$ ratios are about 1/27! It means that only depending on superheated driving Gibbs energy and vibration energy, the A_8^{Au} and A_4^{Cu} alloy genes can not surmount potential barriers to alternate lattice positions, occur splitting and change occupied Gibbs energy levels.

Comparing the equilibrium $x_{i,e}^{\text{Au}} - T$ and $x_{i,e}^{\text{Cu}} - T$ paths on disordering stoichiometric AuCuI ($A_8^{\text{Au}}A_4^{\text{Cu}}$) compound with its experimental $x_{i,s}^{\text{Au}} - T$ and $x_{i,s}^{\text{Cu}} - T$ paths, some discoveries have been obtained. 1) The essential on disordering AuCuI ($A_8^{\text{Au}}A_4^{\text{Cu}}$) compound is that A_8^{Au} and A_4^{Cu} stem alloy genes are split into the A_i^{Au} and A_i^{Cu} sequences in the disordered state. And then the essential on ordering equiatomic AuCu alloy is that the A_i^{Au} and A_i^{Cu} sequences in the disordered states are degenerated into the A_8^{Au} and A_4^{Cu} stem alloy genes in the AuCuI ($A_8^{\text{Au}}A_4^{\text{Cu}}$). 2) It has been discovered that the 3(RA-SA) mechanism of atom movement at the beginning period on disordering AuCuI ($A_8^{\text{Au}}A_4^{\text{Cu}}$) compound is that three AG-pairs in a cell-scale region occur resonance activating to accumulate vibration energies and synchro alternating to change their lattice positions and their probabilities

occupied at the Gibbs energy levels. 3) There exist jumping alloy genes on disordering AuCuI ($A_8^{\text{Au}}A_4^{\text{Cu}}$) compound and their jumping order degrees with maximum emergent phenomenon, which is defined as that their concentrations are larger than the those of the corresponding alloy genes in the disordered state. 4) It has been discovered that the jumping order degree leads to the existence of jumping T_j -temperature and an unexpected so-called “retro-effect” about jumping temperature retrograde shift to lower temperatures upon increasing the heating rate. 5) It has been discovered that a new atom movement mechanism of AuCuI ($A_8^{\text{Au}}A_4^{\text{Cu}}$) to change structure for suiting variation in temperature is the “resonance activating-synchro alternating” of alloy genes, it leads to heterogeneous and successive subequilibrium transitions. 6) It has been discovered that the SPAP-AuCuII alloy containing early-, middle- and late-SPAP-AuCuII regions is a statistic periodic antiphase structure stacking of incommensurate tetragonal cells containing more A_8^{Au} and A_4^{Cu} alloy genes and antiphase boundary $n(\text{RA-SA})$ cells containing less A_8^{Au} and A_4^{Cu} alloy genes along b axis. It has no strict long periodic cell. The number M of cells between two successive antiphase boundaries is only an average, which is about 5. 7) It has been discovered that up to now, researchers have got used to recognizing the experimental phenomena observed during very slow variation in temperature to be thermodynamic equilibrium, lacking an essential definition of the thermodynamic equilibrium order-disorder transition (see Section 3).

5.2 HAPDS-databases

The HAPDS-database is a complex system of scientific–technology–society combination body with multi-levels. Therefore, the HAPDS-databases possess following characteristics.

1) The HAPDS-database possess systematicness, which consists of MC-database of the MC-center, HAK-database of the SMMS-center, AGE-database of the AGE-center, shared information database of the HAPDSI-center and public policy database of the HAPDSC-center (see Fig. 1).

2) The HAPDS-database is commonly established by all parts in the HAPDS-base.

3) The HAPDS-database is shared by all parts in the HAPDS-base.

4) It is emphasized that the HAPDS-database should move in cycle within the all parts in the HAPDS-base, that not only can expand and correct database, but also can increase interconnection of all parts and young vigor of HAPDS-base, and promote control power of the HADSC-center for boosting sustainable progress of systematic metal materials science and alloy gene

engineering.

6 Conclusions

1) The systematic investigation on Au–Cu system is a good paragon for establishing SMMS-framework to be guided by the seven philosophic propositions of systematology, that will prove stimulating to researchers working on general system sciences, matter systems and social systems, and who may well find values in using them as a philosophic thinking logic for establishing various alloy system science frameworks, various matter system science frameworks and various social system science frameworks.

2) To establish HAPDS-system is a good way for boosting sustainable progress of SMMS-framework and AG-engineering, and in order to discover, design, manufacture, deploy and develop advanced alloys in a more expeditious and economical way. Its base is a scientific–technology–society combination system, which should be established under the guide of seven philosophic propositions of systematology.

3) It has been discovered that the RA-SA mechanism is a located atom movement mechanism rather than a oriented diffuse atom movement mechanism in the Au–Cu system. Then, we have predicated the subequilibrium limit composition ranges of the Au₃Cu-, AuCu- and AuCu₃-type LRO alloys, and that the $T_{\Delta G^m} - x$ SHNP diagrams should be established by the cross point numerical method (or differential numerical method) of equilibrium isothermal Gibbs energy $\Delta G_T^m - x$ curves. The calculated results are in good agreement with the experimental phenomena.

4) It has been discovered that the first and second jumping alloy genes and their jumping order degree depend on the compositions of alloys. Therefore, it has been predicated that there exist jumping iso-order degree $\sigma_j(T, x)$ regions in the range $0.6 \leq \sigma_j(T, x) \leq 0.8$. It means that there exist LRO-region, SRO-region and disordered region in the SHNP diagrams of Au–Cu system, which are in good agreement with the experimental phenomena.

5) The EHNP and SHNP diagrams are blueprints and operable platform for researchers to discover, design, manufacture and deploy advanced alloys, which are obtained respectively by the equilibrium lever numerical method and cross point numerical method of isothermal Gibbs energy curves. As clicking each network point, the holographic information of three structure levels for the designed alloy may be readily obtained: the phase constitution and fraction, phase arranging structure and properties of organization; the composition, alloy gene arranging structure and properties of each phase and the electronic structures and properties of alloy genes. It will

create a new era for designing advanced alloys on the network.

Appendixes

A EHNP-and SHNP diagrams of Au–Cu system

A.1 Comparisons of EHNP-and SHNP diagrams of Au–Cu system with CALPHAD- and QMAC-diagrams

Figure A.1 shows the comparisons of EHNP–and SHNP diagrams of Au–Cu system with CALPHAD- and QMAC-diagrams.

1) The ordered phases of Au₃Cu-, AuCu- and AuCu₃-type sublattice systems are separated from the disordered phase by a single $T_c - x$ curve rather than by a two-phase coexisting region in the EHNP- and SHNP-diagrams (Figs. A.1(a) and (b)), that is in agreement with the experimental phenomena [24,47–49]. However, the ordered phase of Au₃Cu-, AuCu- and AuCu₃-type sublattice systems are separated respectively from the disordered phase by two-phase coexisting regions in the CALPHAD- and QMAC-diagrams (Figs. A.1(c)–(f)), that have been never observed in experiments [24,47–49].

2) The highest critical T_c -point on the $T_c - x$ curve of Au–Cu system is located at the network point ($x_{Cu}=55.5\%$, $T_c=839$ K, $\Delta G^m=-10189.02$ J/mol) in the EHNP- and SHNP-diagrams of Au–Cu system. From Fig. A.2, it can be known that the network points of the highest critical points of the Au₃Cu-, AuCu- and AuCu₃-type sublattice systems are respectively $H(x_{Cu}=52.25\%$, $T_c=835$ K, $\Delta G^m=-10219$ J/mol), $H(x_{Cu}=52.80\%$, $T_c=835$ K, $\Delta G^m=-10215.12$ J/mol), $H(x_{Cu}=55.50\%$, $T_c=839$ K, $\Delta G^m=-10189.02$ J/mol). However, the compositions of the highest critical points of the Au₃Cu-, AuCu- and AuCu₃-type sublattice systems are located respectively at the stoichiometric compositions: 25% Cu, 50% Cu and 75% Cu (Figs. A.1(c)–(f)).

3) In the SHNP-diagram (Fig. 5(f), Fig. A.1(b)), the subequilibrium limit composition ranges of the LRO Au₃Cu-, AuCu- and AuCu₃-alloys at 0 K are respectively 18.875%–36.20% Cu, 36.20%–63.05% Cu and 63.05%–81.125% Cu, which are in good agreement with the experimental results at room temperature: 21%–36.8% Cu, 36.8%–62.5% Cu and 62.5%–79.5% Cu [47–49]. However, there is no subequilibrium phase diagram in the CALPHAD- and QMAC- thermodynamics.

4) In the SHNP-diagram, the phase boundary curves between AuCu- and Au₃Cu-type ordered regions and between AuCu- and AuCu₃-type ordered regions are respectively the $[T_{\Delta G^m}(\text{Au}_3\text{Cu - type, AuCu - type}) - x]_{PB}$ curve (left side on Fig. A.1(b)) and the $[T_{\Delta G^m}(\text{AuCu - type, AuCu}_3\text{ - type}) - x]_{PB}$ curves (right

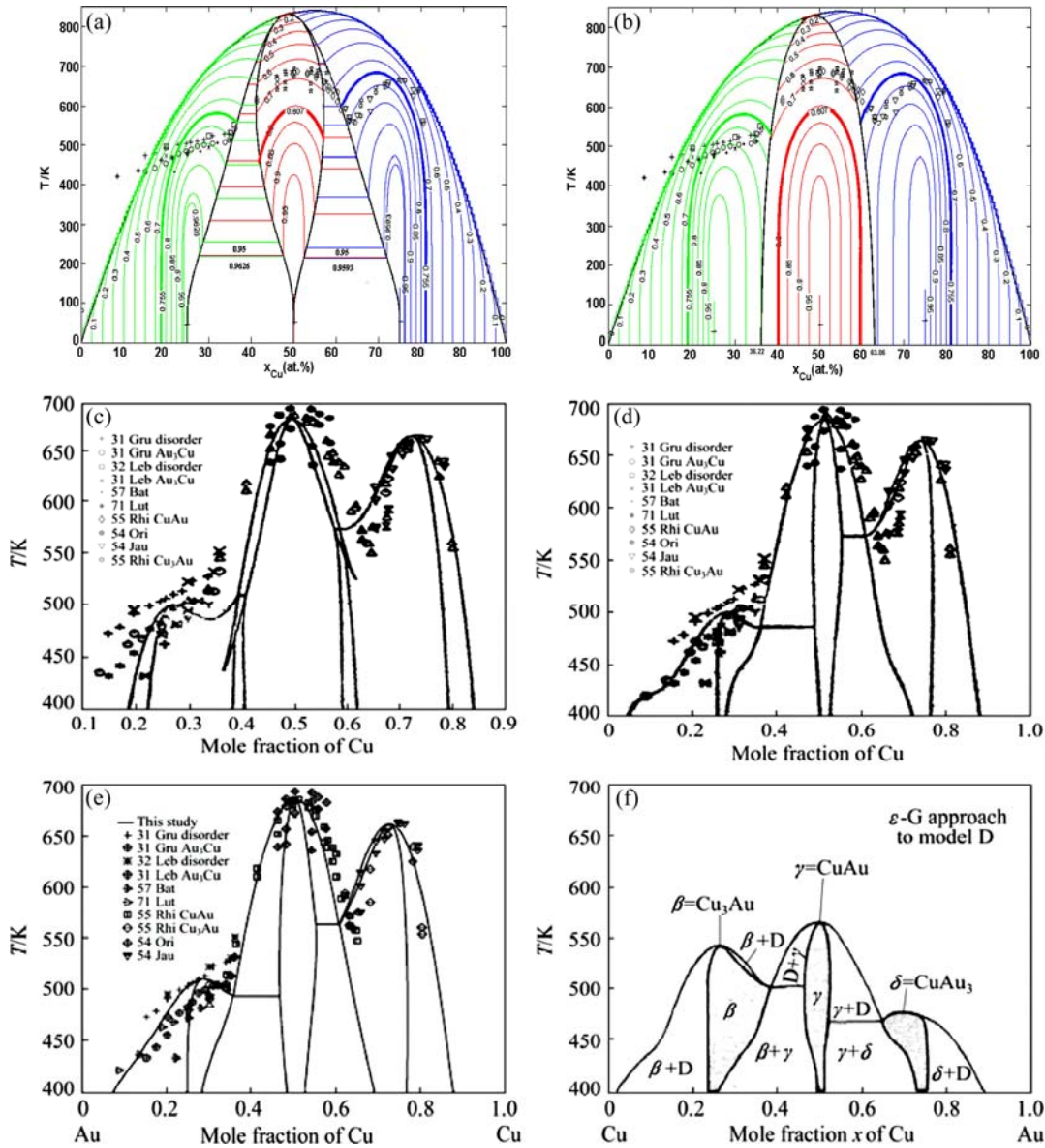


Fig. A.1 EHNP, SHNP, CALPHAD and QMAC diagrams of Au–Cu system: (a) Equilibrium phase diagram with iso-order degree $T_{\sigma} - x$ curves and experimental jumping $T_j(x)$ points; (b) Subequilibrium phase diagram with iso-order degree $T_{\sigma} - x$ curves and experimental jumping $T_j(x)$ points; (c)–(f) CALPHAD-diagram given in Refs. [17], [18], [50] and [51] (The experimental jumping T_j -temperatures, which were erroneously considered as the equilibrium critical T_c -temperatures in Ref. [17])

side on Figs. A.1(b)). However, we also predicated that the phase boundary curves between two ordered phases may be possible to expand into the narrow coexisting phase boundary bands of two ordered phases via proper heat treatment or very-very long ageing at high temperature. Namely, there may be decomposition reaction (see Section 4), that is in agreement with the experimental phenomenon [47–49]. However, there is no subequilibrium phase diagram in the QMAC- and CALPHAD-thermodynamics.

In the SHNP-diagram, there exist jumping $T_{\sigma_j} - x$ regions in the range $0.6 \leq \sigma_j \leq 0.8$. It means that there exist LRO-regions, SRO-regions and disordered region, that are in good agreement with the experimental

phenomena. However, the researchers in the QMAC- and CALPHAD-communities erroneously considered the jumping T_j -temperatures as the selected information of the critical T_c -temperatures, then adjusted parameters in Gibbs energy functions and established so-called equilibrium phase diagrams to achieve the best representation of the selected information [22]. These phase diagrams are questionable in many respects.

The equilibrium and subequilibrium holographic network phase diagrams are blueprints and operable platform for researchers to discover, design, manufacture and deploy advanced alloys, they are obtained respectively by the equilibrium lever numerical method and cross point numerical method of isothermal Gibbs

energy curves. As clicking each network point, the holographic information of three structure levels for the designed alloy may be readily obtained: the phase constitution and fraction, phase arranging structure and properties of organization; the composition, alloy gene arranging structure and properties of each phase and the electronic structures and properties of alloy genes. It will create a new era for network designing advanced alloys.

A.2 Steps to establish EHNP and SHNP diagrams of Au–Cu system

The steps to establish EHNP and SHNP diagrams of Au–Cu system may be illustrated by Fig. A.3.

A.3 Equilibrium holographic network phase (EHNP) diagrams of AuCu-, AuCu₃- and Au₃Cu-type sublattice systems

Based on the AG-holographic information database and essential definition of equilibrium order–disorder transition, the traditional phase diagram of single ordered phase sublattice system described only by phase boundary lines has been developed into a set of EHNP-diagrams described by a set of information about AGA-structures, physical and thermodynamic properties, which are established by the minimum mixed Gibbs energy path method. From Fig. A.2, it can be known that the network points of the highest critical points of the Au₃Cu-, AuCu- and AuCu₃-type sublattice systems

are respectively $H(x_{Cu}=52.25\%, T_c=835\text{ K}, \Delta G^m=-10219\text{ J/mol})$, $H(x_{Cu}=52.80\%, T_c=835\text{ K}, \Delta G^m=-10215.12\text{ J/mol})$, $H(x_{Cu}=55.50\%, T_c=839\text{ K}, \Delta G^m=-10189.02\text{ J/mol})$.

B Equilibrium lever numerical method of isothermal Gibbs energy curves for establishing EHNP-diagrams of Au–Cu system

The solid FCC-based lattice Au–Cu system is a competitive system of the ordered Au₃Cu-, AuCu- and AuCu₃-type sublattice systems and disordered FCC-based lattice Au–Cu system. The three dimensional $\Delta G^m - T - x$ EHNP diagram may be established by the equilibrium lever numerical method of isothermal Gibbs energy curves.

B.1 Equilibrium Gibbs energy lever method in whole composition region

1) Known conditions

Two-dimensional isothermal Gibbs energy $\Delta G_T^m - x$ EHNP diagrams of ordered Au₃Cu-, AuCu- and AuCu₃-type sublattice systems and disordered FCC-based lattice Au–Cu system have been calculated by composition step $\Delta x=0.05\%$ and temperature step $\Delta T=1\text{ K}$ (Fig. B.1).

The isothermal Gibbs energy $\Delta G_T^m - x$ curves of ordered Au₃Cu-, AuCu- and AuCu₃-type sublattice

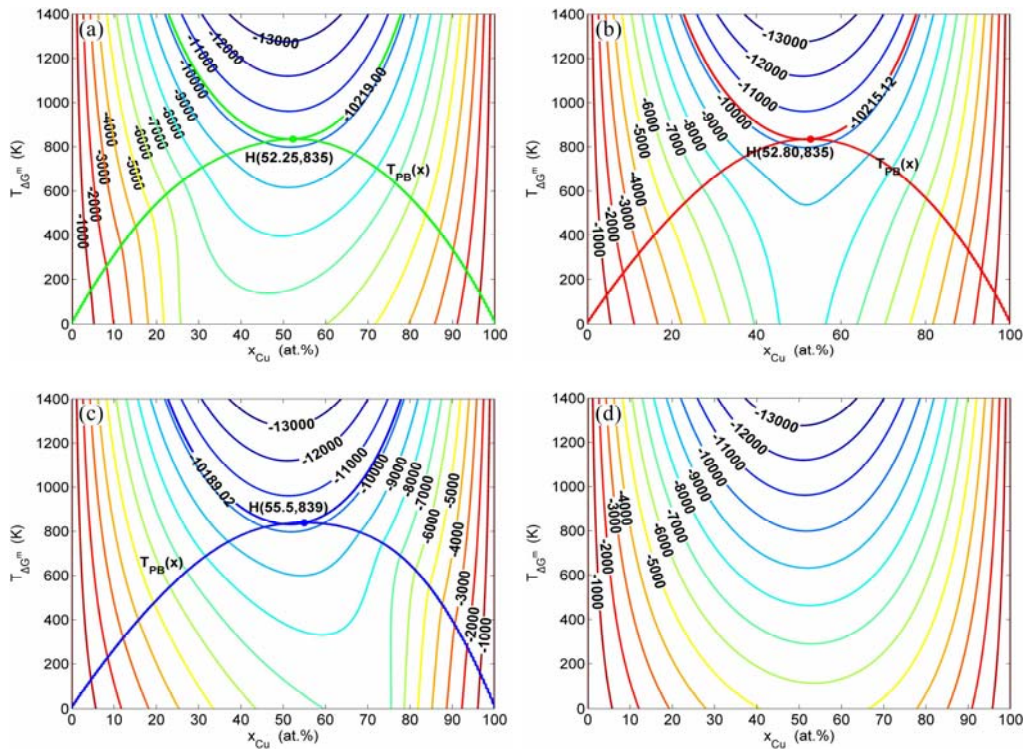


Fig. A.2 Two-dimensional isothermal Gibbs energy $\Delta G_T^m - x$ EHNP diagrams: (a) $T-x$ equilibrium phase diagram with iso-mixed Gibbs energy $T_{\Delta G^m} - x$ curves of Au₃Cu-type sublattice system; (b) $T-x$ equilibrium phase diagram with iso-mixed Gibbs energy $T_{\Delta G^m} - x$ curves of AuCu-type sublattice system; (c) $T-x$ equilibrium phase diagram with iso-mixed Gibbs energy $T_{\Delta G^m} - x$ curves of AuCu₃-type sublattice system; (d) $T-x$ equilibrium phase diagram with iso-mixed Gibbs energy $T_{\Delta G^m} - x$ curves of FCC-based lattice disordered Au_(1-x)Cu_x solution

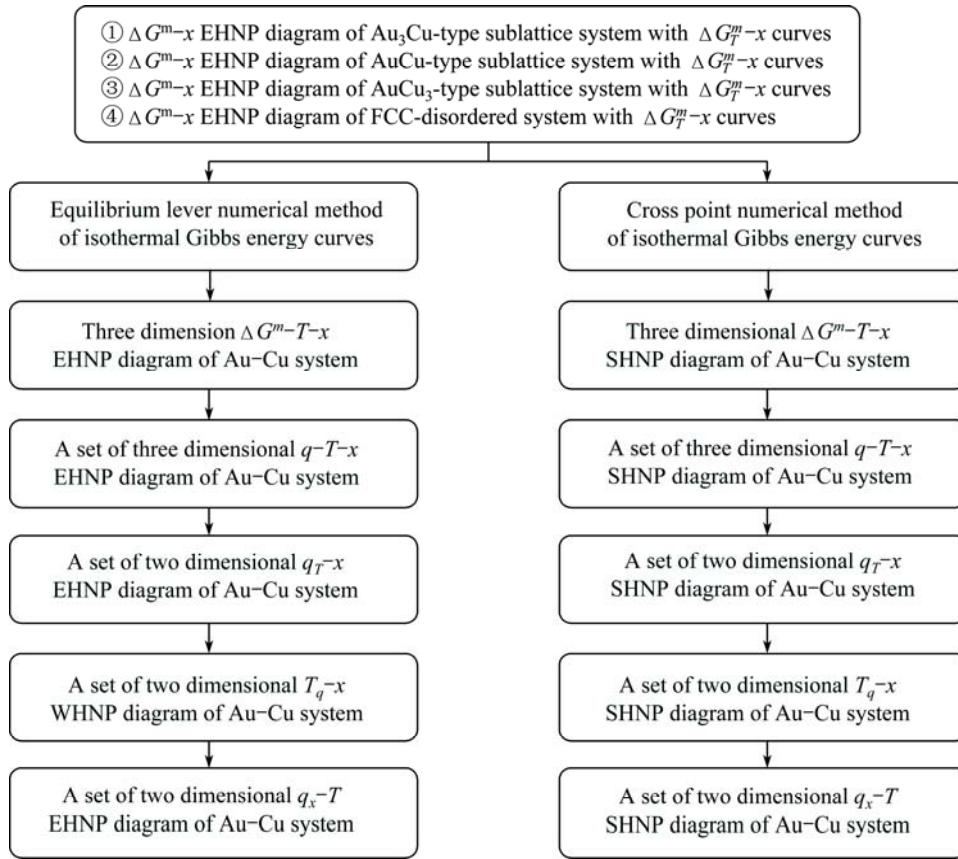


Fig. A.3 Steps to establish EHNP and SHNP diagrams of Au–Cu system (q denote mixed Gibbs energy ΔG^m , order degree σ , configurational entropy S^c , mixed characteristic Gibbs energy ΔG^{*m} , mixed enthalpy ΔH^m , mixed potential energy ΔE^m , mixed volume ΔV^m , generalized vibration free energy X^v , generalized vibration energy U^v , generalized vibration entropy S^v , mixed specific heat capacity Δc_p^m , mixed thermal expansion coefficient $\Delta \alpha^m$ and activities (a_{Au} and a_{Cu}))

systems and disordered FCC-based lattice Au–Cu system at a given T -temperature have been established. The isothermal $\Delta G_{A,T}^m-x$ and $\Delta G_{B,T}^m-x$ curves have 2001 numerical points, respectively, where A and B may represent two different order sublattice systems (Fig. B.2).

At a given T -temperature, there are $(2001)^2=4004001$ ($\Delta G_A^m(T, x_a) - \Delta G_B^m(T, x_b)$) connection lines. But only one may be the equilibrium Gibbs energy ($\Delta G_A^m(T, x_A) - \Delta G_B^m(T, x_A)$) lever between the $\Delta G_A^m(T, x)$ and $\Delta G_B^m(T, x)$ curves (Fig. B.2).

2) Equations

Gibbs energy equation of the “tracer alloy” on the ($\Delta G_A^m(T, x_a) - \Delta G_B^m(T, x_b)$) connection lines (see Fig. B.2):

$$\Delta G_{A,B}^m(T, x_c) = \frac{x_b - x_c}{x_b - x_a} \times \Delta G_A^m(T, x_a) - \frac{x_c - x_a}{x_b - x_a} \times \Delta G_B^m(T, x_b) \tag{B.1}$$

Gibbs energy equation of the “tracer alloy” with minimum Gibbs energy on the equilibrium ($\Delta G_A^m(T, x_A) - \Delta G_B^m(T, x_B)$) lever (see Fig. B.2):

$$(\Delta G_{A,B}^m(T, x_c))_{\min} = \frac{x_B - x_c}{x_B - x_A} \times \Delta G_A^m(T, x_A) - \frac{x_c - x_A}{x_B - x_A} \times \Delta G_B^m(T, x_B) \tag{B.2}$$

where the composition x_c of the tracer alloy consisting of A and B phases may be any point between x_A and x_B points, it can be easily determined by inspection. By this method, the three-dimensional ΔG^m-T-x EHNP diagrams may be established. Then, a set of three-dimensional $q-T-x$ EHNP diagrams, two-dimensional q_T-x , T_q-x and q_x-T EHNP diagram may be established. It should be pointed out that this method can not only determine the equilibrium phase boundary covers of ordered AuCu-sublattice system with ordered Au_3Cu - and $AuCu_3$ -sublattice system, but also can demonstrate that there is no a two-phase region between disordered and ordered phases in the Au–Cu system.

B.2 Equilibrium Gibbs energy lever method in a selected composition region

1) Known conditions

Two-dimensional isothermal Gibbs energy ΔG_T^m-x

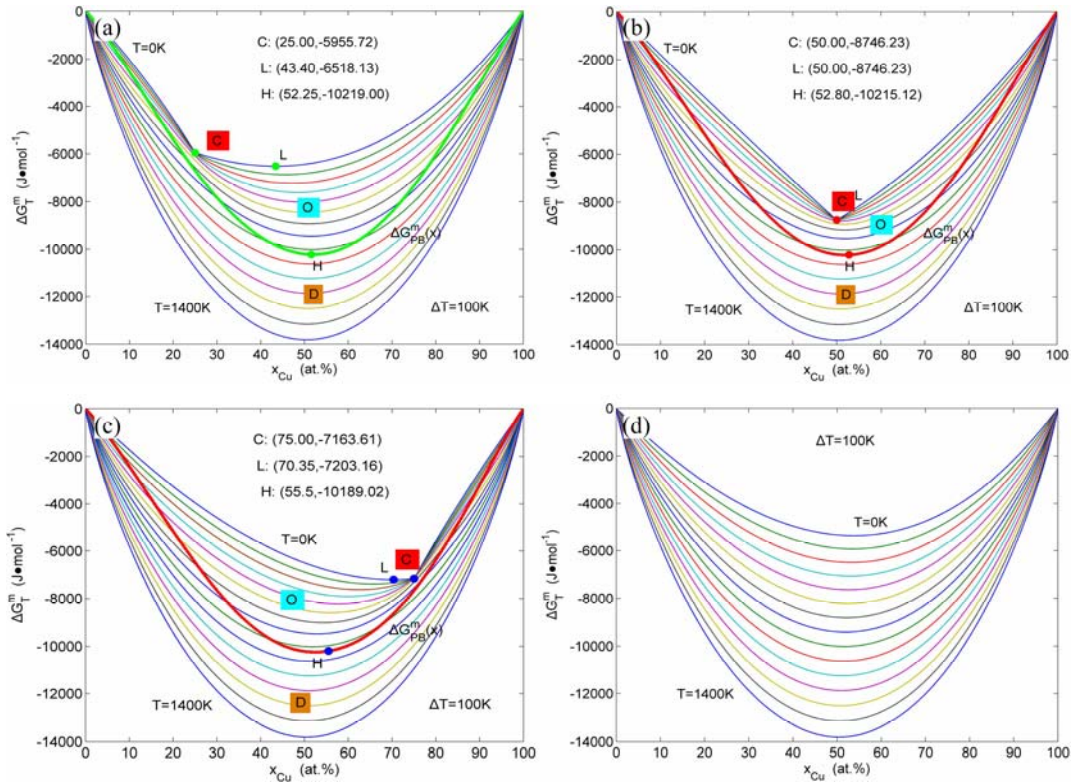


Fig. B.1 Two-dimensional isothermal Gibbs energy $\Delta G_T^m - x$ EHP diagrams: (a) $\Delta G^m - x$ equilibrium phase diagram of Au_3Cu -type sublattice system with isothermal $\Delta G_T^m - x$ diagram and phase boundary curve $\Delta G_{PB}^m(x)$; (b) $\Delta G^m - x$ equilibrium phase diagram of $AuCu$ -type sublattice system with isothermal $\Delta G_T^m - x$ diagram and phase boundary curve $\Delta G_{PB}^m(x)$; (c) $\Delta G^m - x$ equilibrium phase diagram of $AuCu_3$ -type sublattice system with isothermal $\Delta G_T^m - x$ diagram and phase boundary curve $\Delta G_{PB}^m(x)$; (d) $\Delta G^m - x$ equilibrium phase diagram of FCC-based lattice disordered $Au_{(1-x)}Cu_x$ solution with isothermal $\Delta G_T^m - x$ diagram (These diagrams are drawn up by composition step $\Delta x=0.05\%$, and temperature step $\Delta T=100$ K. the symbols “O”, “D”, “C”, “L” and “H” denote respectively ordered region, disordered region, stoichiometric compound, lowest network point at 0 K and the lowest network point on the phase boundary curve)

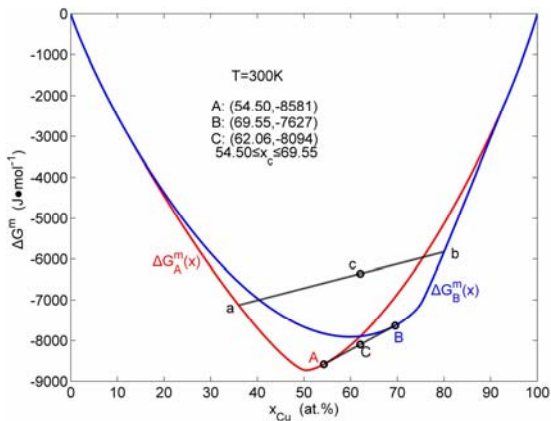


Fig. B.2 Equilibrium lever numerical method of whole composition region ($\Delta G_A^m(x)$ and $\Delta G_B^m(x)$ are respectively isothermal mixed Gibbs energy curves of $AuCu$ - and $AuCu_3$ -type ordered phases as function of composition at 300 K. $A-C-B$ line is the equilibrium lever of $AuCu$ - and $AuCu_3$ -type ordered alloys)

EHP diagrams of ordered Au_3Cu -, $AuCu$ - and $AuCu_3$ -type sublattice system and disordered FCC-based lattice $Au-Cu$ system have been calculated by composition step

$\Delta x = \varepsilon = 0.05\%$ and temperature step $\Delta T=1$ K (Fig. B.1).

The isothermal Gibbs energy $\Delta G_T^m - x$ curves of ordered Au_3Cu -, $AuCu$ - and $AuCu_3$ -type sublattice systems and disordered FCC-based lattice $Au-Cu$ system at a given T -temperature have been established. The isothermal $\Delta G_{A,T}^m - x$ and $\Delta G_{B,T}^m - x$ curves have 2001 numerical points, respectively, where, A and B may represent two different order sublattice systems.

The selected region may be easily determined by inspection, of which the composition range is 50%–75% Cu at 300 K (Fig. B.3). The $\Delta G_{A,T}^m - x$ and $\Delta G_{B,T}^m - x$ curves have 500 numerical points, respectively, where, A and B represent $AuCu$ - and $AuCu_3$ -type sublattice systems. Therefore, there are $(501)^2=251001$ connection lines, which are much less than those of equilibrium Gibbs energy lever method in the whole composition. For an experienced researcher, these connection lines may be much reduced.

At a given T -temperature, the composition (x_c) of the cross point between $\Delta G_{A,T}^m - x$ and $\Delta G_{B,T}^m - x$ curves may be determined by equation (Fig. B.3):

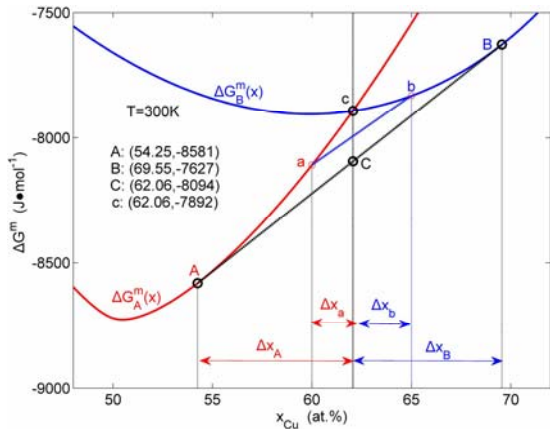


Fig. B.3 Equilibrium lever numerical method in a selected composition region ($\Delta G_A^m(x)$ and $\Delta G_B^m(x)$ are respectively isothermal mixed Gibbs energy curves of AuCu- and AuCu₃-type ordered phases as function of composition at 300 K. $A-C-B$ line is the equilibrium lever of AuCu- and AuCu₃-type ordered alloys)

$$\Delta G_{A,T}^m(x_c) - \Delta G_{B,T}^m(x_c) = 0 \tag{B.3}$$

The x_c -composition is selected as the tracer alloy.

2) Equations

Gibbs energy equation of the “tracer alloy” on the ($\Delta G_A^m(x_a) - \Delta G_B^m(x_b)$) connection lines (Fig. B.3):

$$\Delta G_{A,B}^m(T, x_c) = \frac{(x_c + \Delta x_b) - x_c}{(\Delta x_a + \Delta x_b)} \times \Delta G_A^m(T, (x_c - \Delta x_a)) - \frac{x_c - (x_c - \Delta x_a)}{(\Delta x_a + \Delta x_b)} \times \Delta G_B^m(T, (x_c + \Delta x_b)) \tag{B.4}$$

Gibbs energy equation of the “tracer alloy” on the equilibrium ($\Delta G_A^m(T, x_A) - \Delta G_B^m(T, x_B)$) lever:

$$(\Delta G_{A,B}^m(T, x_c))_{\min} = \frac{(x_C + \Delta x_B) - x_C}{\Delta x_A + \Delta x_B} \times \Delta G_A^m(T, (x_C - \Delta x_A)) - \frac{x_C - (x_C - \Delta x_A)}{\Delta x_A + \Delta x_B} \times \Delta G_B^m(T, (x_C + \Delta x_B)) \tag{B.5}$$

C Cross point numerical method of isothermal Gibbs energy curves for establishing SHNP-diagrams of Au–Cu system

The cross point numerical method of isothermal Gibbs energy curves may be described by differential values of isothermal Gibbs energy curves. Therefore, this method may be also called as the differential method of isothermal Gibbs energy curves. In the present work, the disordered alloys are taken as the standard. The SHNP-diagrams of Au–Cu system established by this method may be illustrated by Figs. C.1 to C.3.

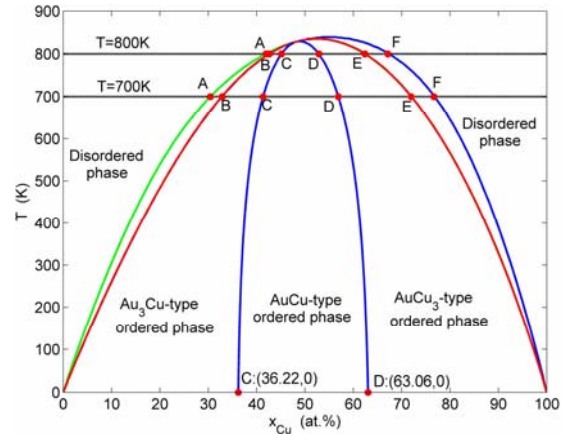


Fig. C.1 Overall aspect of cross point numerical method for establishing SHNP-diagrams of Au–Cu system

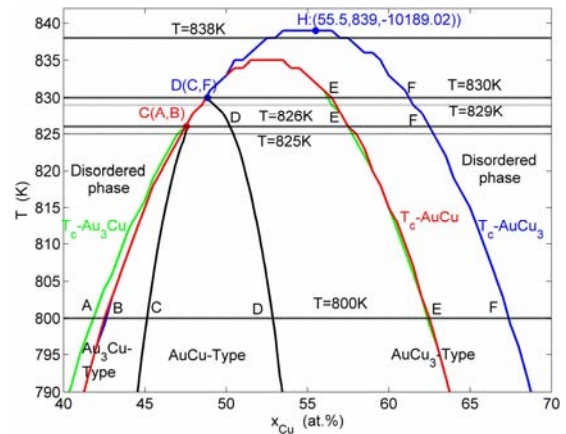


Fig. C.2 Top part of cross point numerical method for establishing SHNP-diagrams of Au–Cu system (The symbols are explained as: A , cross point of isothermal Gibbs energy curves of ordered Au₃Cu-type phase and disordered FCC-alloy phase; B , cross point of isothermal Gibbs energy curves of ordered AuCu-type phase and disordered FCC-alloy phase; C , cross point of isothermal Gibbs energy curves of ordered Au₃Cu-type and AuCu-type phase; D , cross point of isothermal Gibbs energy curves of ordered AuCu-type and AuCu₃-type phase; E , cross point of isothermal Gibbs energy curves of ordered AuCu-type (Au₃Cu-type) and disordered FCC-alloy phase; F , cross point of isothermal Gibbs energy curves of ordered AuCu₃-type phase and disordered FCC-alloy phase; $C(A,B)$, common point reaction of Au₃Cu-type, AuCu-type and disordered FCC-alloy phase; $D(C,F)$, common point reaction of AuCu-type, AuCu₃-type and disordered FCC-alloy phase; H , the highest critical T_c -point on the $T_c - x$ curve of Au-Cu system)

From Figs. C.1 and C.2, we can obtain the following knowledges:

The phase boundary curve $T_c - x$ between the ordered and disordered phases consists of three line segments: the $O-A-A-C(A,B)$ line segment (see Figs. C.1 and C.2) between Au₃Cu-type ordered and

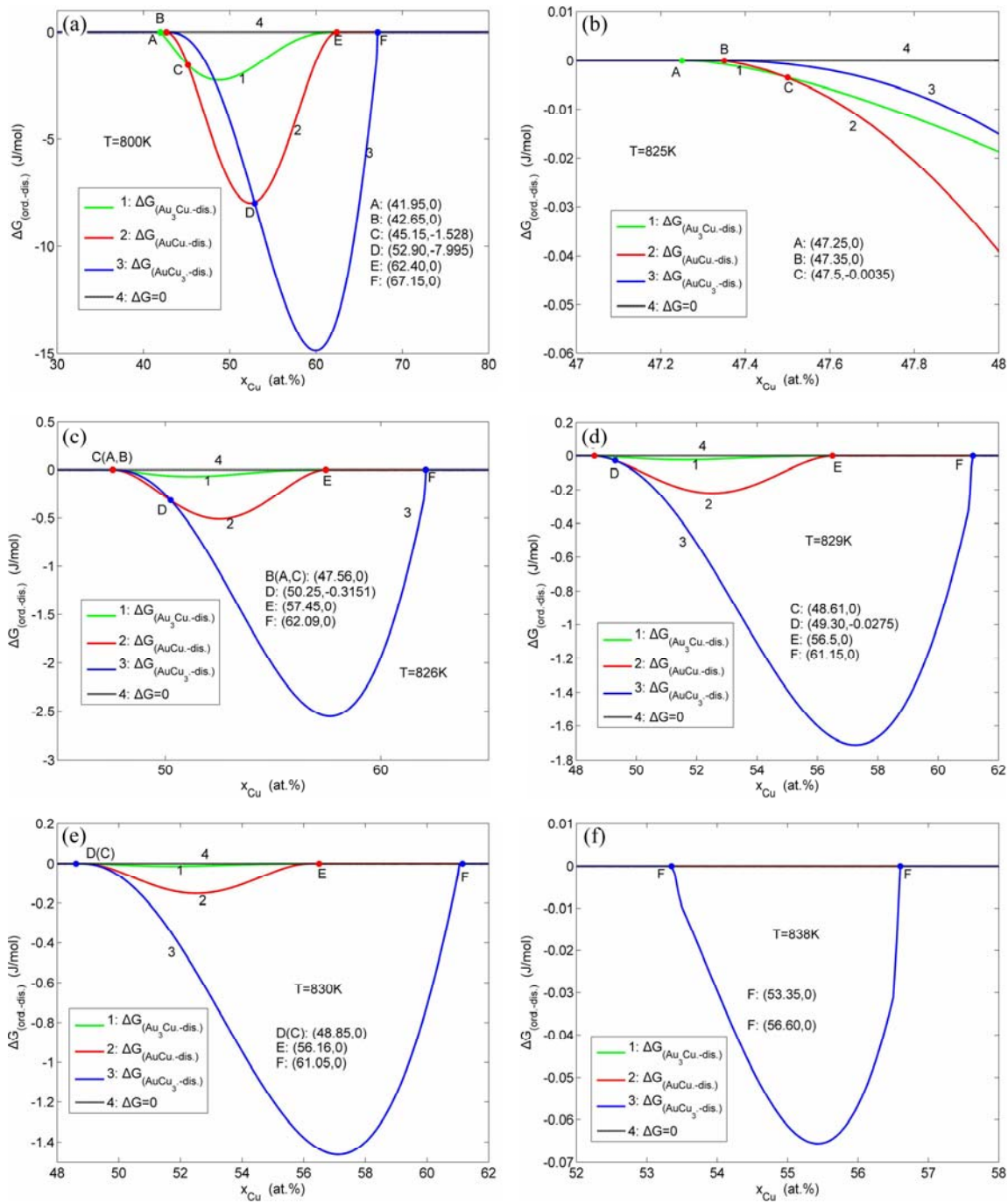


Fig. C.3 Analysis of cross points at 800, 825, 826, 829, 830 and 838 K

disordered phases, $C(A,B) - D(C,F)$ line segment (see Fig. C.2) between AuCu-type ordered and disordered phases, and $D(C,F) - H - F - F$ line segment between AuCu₃-type ordered and disordered phases.

The $C - C - C - C(A,B)$ curve (see Figs. C.1 and C.2) is the phase boundary curve between Au₃Cu-type and AuCu-type ordered phases, which may be described by the $[T_{\Delta G^m}(Au_3Cu - type, AuCu - type) - x]_{PB}$ curve (see Section 4).

The $D - D - D - D(C,F)$ curve (see Figs. C.1 and C.2) is the phase boundary curve between AuCu-type

and AuCu₃-type ordered phases, which may be described by the $[T_{\Delta G^m}(AuCu - type, AuCu_3 - type) - x]_{PB}$ curve (see Section 4).

The highest critical T_c -point on the $T_c - x$ curve of Au–Cu system is located at the network point ($x_{Cu} = 55.5\%$, $T_c = 839$ K, $\Delta G^m = -10189.02$ J/mol), through accurate calculation by the differential method between Gibbs energies of ordered and disordered alloys. The analysis of cross points at 800 K (see Fig. C.3(a), Table C.1), 825, 826, 829, 830 and 838 K is shown in Fig. C.3 and Table C.1.

Table C.1 Differential values of Gibbs energies of Au₃Cu-, AuCu- and AuCu₃-type alloys at 800 K, taking $\Delta G_{\text{dis}}^{\text{m}} - x$ curve as standard (see Fig. C.3(a))

$x_{\text{Cu}} / \%$	$\Delta G_{(\text{Au}_3\text{Cu-dis})}^{\text{m}} / (\text{J}\cdot\text{mol}^{-1})$	$\Delta G_{(\text{AuCu-dis})}^{\text{m}} / (\text{J}\cdot\text{mol}^{-1})$	$\Delta G_{(\text{AuCu}_3\text{-dis})}^{\text{m}} / (\text{J}\cdot\text{mol}^{-1})$	$x_{\text{Cu}} / \%$	$\Delta G_{(\text{AuCu-dis})}^{\text{m}} / (\text{J}\cdot\text{mol}^{-1})$	$\Delta G_{(\text{AuCu}_3\text{-dis})}^{\text{m}} / (\text{J}\cdot\text{mol}^{-1})$	$\Delta G_{(\text{Au}_3\text{Cu-dis})}^{\text{m}} / (\text{J}\cdot\text{mol}^{-1})$
40.500	0	0	0	55.00	-0.9956	-6.8920	-10.9088
41.00	0	0	0	55.50	-0.8617	-6.4535	-11.5545
41.50	0	0	0	56.00	-0.7332	-5.9588	-12.1666
41.95(A))	0	0	0	56.50	-0.6118	-5.4174	-12.7370
42.00	-0.0152	0	0	57.00	-0.4991	-4.8400	-13.2578
42.50	-0.2308	0	0	57.50	-0.3964	-4.2384	-13.7205
42.65(B)	-0.3042	0	0	58.00	-0.3049	-3.6250	-14.1167
43.00	-0.4827	-0.0396	-0.0016	58.50	-0.2255	-3.0135	-14.4376
43.50	-0.7433	-0.2123	-0.0182	59.00	-0.1586	-2.4179	-14.6745
44.00	-0.9982	-0.5045	-0.0633	59.50	-0.1044	-1.8530	-14.8186
44.50	-1.2383	-0.8974	-0.1457	60.00	-0.0628	-1.3344	-14.8610
45.00	-1.4577	-1.3724	-0.2707	60.50	-0.0331	-0.8777	-14.7931
45.15(C)	-1.5188	-1.5282	-0.3171	61.00	-0.0141	-0.4994	-14.6064
45.50	-1.6522	-1.9113	-0.4421	61.50	-0.0040	-0.2162	-14.2928
46.00	-1.8196	-2.4967	-0.6620	62.00	-0.0004	-0.0449	-13.8447
46.50	-1.9583	-3.1116	-0.9314	62.40(E)	0	0	-13.3846
47.00	-2.0679	-3.7400	-1.2505	62.50	0	0	-13.2551
47.50	-2.1485	-4.3665	-1.6185	63.00	0	0	-12.5181
48.00	-2.2008	-4.9768	-2.0341	63.50	0	0	-11.6292
48.50	-2.2260	-5.5578	-2.4954	64.00	0	0	-10.5854
49.00	-2.2255	-6.0974	-2.9997	64.50	0	0	-9.3860
49.50	-2.2012	-6.5848	-3.5442	65.00	0	0	-8.0332
50.00	-2.1549	-7.0107	-4.1253	65.50	0	0	-6.5333
50.50	-2.0889	-7.3671	-4.7393	66.00	0	0	-4.8975
51.00	-2.0054	-7.6475	-5.3817	66.50	0	0	-3.1450
51.50	-1.9068	-7.8469	-6.0479	67.00	0	0	-1.3062
52.00	-1.7955	-7.9621	-6.7328	67.15(F)	0	0	0
52.90(D)	-1.5709	-7.9522	-7.9953	67.50	0	0	0
52.50	-1.6739	-7.9911	-7.4310	68.00	0	0	0
53.00	-1.5445	-7.9339	-8.1368	68.50	0	0	0
53.50	-1.4097	-7.7917	-8.8441	69.00	0	0	0
54.00	-1.2717	-7.5675	-9.5464	69.50	0	0	0
54.50	-1.1330	-7.2657	-10.2370	70.00	0	0	0

References

- [1] XIE You-qing. A review and thinking of materials design [J]. Materials Review, 1995, 9(2): 1–7. (in Chinese)
- [2] XIE You-qing. Development course of metallic materials science and evolution of human thinking mode [J]. Materials Review, 1998, 12(4): 6–10. (in Chinese)
- [3] XIE You-qing. Systematic science of alloys [M]. Changsha: Central South University Press, 2012: 3–25.
- [4] SLATER J C. Electronic structure of alloys [J]. Journal of Applied Physics, 1937, 8(6): 385–396.
- [5] ELLIS D E, AVERRILL F W. Electronic structure of FeCl₄ anions in the Hartree-Fock-Slater model [J]. J Chem Phys, 1974, 60(8): 2856–2864.
- [6] BAERENDS E J, ELLIS D E, ROS P. Self-consistent molecular Hartree-Fock-Slater calculations. I. The computational procedure [J]. Chem Phys, 1973, 2(1): 41–51.
- [7] KIKUCHI R. A theory of cooperative phenomena [J]. Phys Rev, 1951, 81(6): 988–1003.
- [8] KIKUCHI R, de FONTAINE D, MURAKAMI M, NAKAMURA T.

- Ternary phase diagram calculations—II. Examples of clustering and ordering systems [J]. *Acta Metallurgica*, 1997, 25(2): 207–219.
- [9] ASTA M, de FONTAINE D. First-principles study of phase stability of Ti–Al intermetallic compounds [J]. *J Mater Res*, 1993, 8(10): 2554–2568.
- [10] OATES W A, ZHANG F, CHEN S L, CHANG Y A. Improved cluster-site approximation for the entropy of mixing in multicomponent solid solutions [J]. *Physical Review B*, 1999, 59(17): 11221–11225.
- [11] OZOLINŠ V, WOLVERTON C, ZUNGER A. Cu–Au, Ag–Au, Cu–Ag and Ni–Au intermetallics: First-principles study of temperature-composition phase diagrams and structures [J]. *Physical Review B*, 1998, 57(12): 6427–6443.
- [12] BRAGG W L, F R S, WILLIAMS E J. The effect of thermal agitation on atomic arrangement in alloys [J]. *Proceedings of the Royal Society A*, 1934, 145(2): 699–730.
- [13] BRAGG W L, WILLIAMS E J. The effect of thermal agitation on atomic arrangement in alloys II [J]. *Proceedings of the Royal Society A*, 1935, 51(2): 540–566.
- [14] ORIANI R A. Thermodynamics of order alloy—II. The gold–copper system [J]. *Acta Metall*, 1954, 2(3): 608–615.
- [15] RHINES F N, BOND W E, RUMMEL R A. Constitution of order alloys of the system copper-gold [J]. *Trans Amer Soc Met*, 1955, 47(2): 578–597.
- [16] KAUFMAN L, BERNSTEIN H. Computer calculation of phase diagrams [M]. Academic Press, New York, 1970: 225.
- [17] SUNDMAN B, FRIES S G, OATES W A. A Thermodynamic assessment of the Au–Cu system [J]. *CALPHAD*, 1998, 22(3): 335–354.
- [18] SUNDMAN B, FRIES S G, OATES W A. A calphad assessment of the Au–Cu system using the cluster variation method [J]. *Z Metallkd*, 1999, 90(5): 267–273.
- [19] HILLERT M. The compound energy formalism [J]. *Journal of Alloys and Compounds*, 2001, 320(1): 161–176.
- [20] OATES W A. Configurational entropies of mixing in solid alloys [J]. *J of Equilibria of Diffusion*, 2007, 28(1): 79–89.
- [21] OSTP. Materials genome initiative for global competitiveness [R]. Washington DC: Office of Science and Technology Policy, 2011.
- [22] KAUFMAN L, ÅGREN J. First and second generation-birth of the materials genome [J]. *Scripta Materialia*, 2014, 70(1): 3–6.
- [23] SUTCLIFFE C H, JAUMOT F E Jr. Order-disorder in Au–Cu alloy—I. Short-range order in an alloy containing atomic percent Au [J]. *Acta Metallurgica*, 1953, 1(2): 725–730.
- [24] JAUMOT F E Jr, SUTCLIFFE C H. Order-disorder in Au–Cu alloy—II. The nature of the order-disorder transformation and long-range order [J]. *Acta Metallurgica*, 1954, 2(2): 63–74.
- [25] SCOTT R E. New complex phase in the copper-gold system [J]. *Journal of Applied Physics*, 1960, 31(12): 2112–2117.
- [26] LANG H, UZAWA H, MOHI T, PFEILER W. L₁₂-long-range order in Cu₃Au: Kinetics and equilibrium as studied by residual resistivity [J]. *Intermetallics*, 2001, 9(1): 9–24.
- [27] KEATING D T, WARREN B E. Long-range order in beta-brass and Cu₃Au [J]. *Journal of Applied Physics*, 1954, 22(3): 286–290.
- [28] BUTLER B D, COHEN J B. The structure of Cu₃Au above the critical temperature [J]. *J Applied Physics*, 1989, 65(6): 2214–2219.
- [29] XIE You-qing, LIU Xin-bi, LI Xiao-bo, PENG Hong-jian, NIE Yao-zhuang. Potential energies of characteristic atoms on basis of experimental heats of formation of AuCu and AuCu₃ compounds [J]. *Transactions of Nonferrous Metals Society of China*, 2009, 19(5): 1243–1256.
- [30] XIE You-qing, LIU Xin-bi, LI Xiao-bo, PENG Hong-jian, NIE Yao-zhuang. Volume sequences of characteristic atoms separated from experimental volumes of AuCu and AuCu₃ compounds [J]. *Transactions of Nonferrous Metals Society of China*, 2009, 19(6): 1599–1617.
- [31] XIE You-qing, NIE Yao-zhuang, LIU Xin-bi, LI Xiao-bo, PENG Hong-jian, LI Yan-fen. Potential energies of characteristic atoms separated from first-principles calculated heats of formation of AuCu and AuCu₃ compounds [C]//XIE You-qing. *Systematic Science of Alloys*. Changsha: Central South University Press, 2012: 405–427.
- [32] XIE You-qing, NIE Yao-zhuang, LIU Xin-bi, LI Xiao-bo, PENG Hong-jian, LI Yan-fen. Volumes of characteristic atoms separated from first-principles calculated volumes of L₁₀-AuCu and L₁₂-AuCu₃ compounds [C]//XIE You-qing. *Systematic Science of Alloys*. Changsha: Central South University Press, 2012: 428–460.
- [33] XIE You-qing. Atomic energies and Gibbs energy functions of Ag–Cu alloys [J]. *Science in China (Series E)*, 1998, 41(2): 146–156.
- [34] XIE You-qing, ZHANG Xiao-dong. Atomic volume and volume functions of Ag–Cu alloys [J]. *Science in China (Series E)*, 1998, 41(2): 157–168.
- [35] XIE You-qing. A new potential function with many-atom interactions in solid [J]. *Science in China (Series E)*, 1993, 36(1): 90–99.
- [36] XIE You-qing. Electronic structure and properties of pure iron [J]. *Acta Metal Mater*, 1994, 42(11): 3705–3715.
- [37] XIE You-qing, LI Xiao-bo, LIU Xin-bi, NIE Yao-zhuang, PENG Hong-jian. Alloy gene Gibbs energy partition function and equilibrium holographic network phase diagrams of AuCu-type sublattice system [J]. *International Journal of Communications, Network and System Sciences*, 2013, 12(6): 415–442.
- [38] XIE You-qing, NIE Yao-zhuang, LI Xiao-bo, PENG Hong-jian, LIU Xin-bi. Alloy gene Gibbs energy partition function and equilibrium holographic network phase diagrams of Au₃Cu-type sublattice system [J]. *Transactions of Nonferrous Metals Society of China*, 2015, 25(1): 211–240.
- [39] XIE You-qing, LI Xiao-bo, LIU Xin-bi, NIE Yao-zhuang, PENG Hong-jian. Alloy gene Gibbs energy partition function and equilibrium holographic network phase diagrams of AuCu₃-type sublattice system [J]. *Transactions of Nonferrous Metals Society of China*, 2014, 24(11): 3585–3610.
- [40] XIE You-qing, PENG Hong-jian, LIU Xin-bi, LI Xiao-bo, NIE Yao-zhuang. New atom movement mechanism for tracking path on disordering AuCu(*A*₃^{Au}*A*₄^{Cu}) compound [J]. *Transactions of Nonferrous Metals Society of China*, 2014, 24(10): 3221–3256.
- [41] XIE You-qing, LIU Xin-bi, PENG Hong-jian, NIE Yao-zhuang, LI Xiao-bo, LI Yan-fen. Characteristic atom arranging crystallography of alloy phases for Au–Cu system [J]. *Science China: Technological Sciences*, 2011, 54(6): 1560–1567.
- [42] XIE You-qing, LI Yan-fen, LIU Xin-bi, LI Xiao-bo, PENG Hong-jian, NIE Yao-zhuang. Characteristic atom occupation patterns of Au₃Cu, AuCu₃, AuCuI and AuCuII based on experimental data of disordered alloys [J]. *Transactions of Nonferrous Metals Society of China*, 2011, 21(5): 1092–1104.
- [43] XIE You-qing, PENG Kun, LIU Xin-bi. Influences of *x*_{Ti}/*x*_{Al} atomic states, lattice constants and potential-energy planes of ordered fcc TiAl type alloys [J]. *Physica B*, 2004, 344(1–4): 5–20.
- [44] XIE You-qing, LIU Xin-bi, PENG Kun. Atomic state, potential energies, volumes, stability and brittleness of ordered fcc TiAl₃ type alloys [J]. *Physica B*, 2004, 353(1–2): 15–33.
- [45] XIE You-qing, PENG Hong-jian, LIU Xin-bi, PENG Kun. Atomic state, potential energies, volumes, stability and brittleness of ordered fcc Ti₃Al type alloys [J]. *Physica B*, 2005, 362(1–4): 1–17.
- [46] XIE You-qing, TAO Hui-jin, PENG Hong-jian, LIU Xin-bi, PENG Kun. Atomic state, potential energies, volumes, stability and brittleness of ordered fcc TiAl₂ type alloys [J]. *Physica B*, 2005, 366: 17–37.
- [47] LU H S, LIANG C K. The superlattice formation and lattice spacing changes in copper-gold alloys [J]. *Acta Physica Sinica*, 1966, 22(6): 659–696. (in Chinese)

- [48] LU H S, LIANG C K. The existence of the superlattice CuAu₃ in the Cu–Au system [J]. Chinese Science Bulletin, 1966, 17(9): 395–396.
- [49] LU H S, LIANG C K. Experimental evidence of order-disorder transitions as of the second degree [J]. Chinese Science Bulletin, 1966, 17(10): 441–443.
- [50] CAO W, CHANG Y A, ZHU J, CHEN S, OATES W A. Thermodynamic modeling of the Cu–Ag–Au system using the cluster/site approximation [J]. Intermetallics, 2007, 15(8): 1438–1446.
- [51] WEI S H, MBAYE A A, FERRIRA L G, ALEX Zun-ger. First-principles calculations of the phase diagrams of noble metals: Cu–Au, Cu–Ag and Ag–Au [J]. Phys Rev B, 1987, 36(20): 4163–4185.

全息合金定位设计系统和 Au–Cu 系的全息网格相图

谢佑卿^{1,2,3}, 刘心笔^{1,2,3}, 李小波⁴, 彭红建⁵, 聂耀庄⁶

1. 中南大学 材料科学与工程学院, 长沙 410083;
2. 中南大学 粉末冶金研究院, 长沙 410083;
3. 中南大学 粉末冶金国家重点实验室, 长沙 410083;
4. 湘潭大学 材料科学与工程学院, 湘潭 411105;
5. 中南大学 化学化工学院, 长沙 410083;
6. 中南大学 物理与电子学院, 长沙 410083

摘要: 以 Au–Cu 系为例, 介绍 3 项发现和 2 个方法。第一, 建立全息合金定位设计系统是推动系统金属材料科学和合金基因工程持续发展的新路径。它的基地由材料测试和计算中心、系统金属材料科学中心、合金基因工程中心、全息合金定位设计系统信息中心和控制中心组成。第二, 原子移动的共振激活和同步交换机制具有 2 种形式: 局域式和定向扩散式。第三, 平衡和亚平衡全息网格相图是研究者发现、设计、生产和应用先进合金的蓝图和可操作平台, 它们分别由合金相的等温 Gibbs 能线的平衡杠杆线数值法和亚平衡交点数值法获得。点击每一格点便可获得设计合金的 3 个结构层次信息: 组织的相的组成和分数, 相的排列结构和性质; 合金相的成分, 合金基因排列结构和性质; 合金基因的电子结构和性质。它将开创一个网络设计先进合金的新时代。

关键词: Au–Cu 系; 全息合金定位设计系统; 平衡和亚平衡全息网络相图; 系统金属材料科学; 网络设计合金

(Edited by Yun-bin HE)